

ON SYNCHRONIZATION IN COUPLED DYNAMICAL SYSTEMS ON HYPERGRAPHS

ANIRBAN BANERJEE & SAMIRON PARUI

*Department of Mathematics and Statistics, Indian Institute of Science Education and Research Kolkata,
Mohanpur-741246, India,*

ABSTRACT. Being cognizant of the abundance of multi-body interactions in various complex systems, we introduce an archetype of dynamical networks. Adopting hypergraph as the underlying architecture aids our proposed dynamical network models to go beyond the traditional archetype of only pair-wise interaction. Besides assimilating the higher-order interactions, the models are flexible enough to comprehend the pair-wise interactions. Consequently, the conventional concept of dynamical networks with graph topology becomes a subcategory of our proposed notion. We introduce some matrices to incorporate the diffusive influence of underlying hypergraphs in dynamical networks. We study global and local synchronization in coupled (discrete and continuous) dynamical systems on (weighted and un-weighted) hypergraphs. We prove that some results on the synchronization in conventional dynamical networks also hold for the same in coupled dynamical systems on hypergraphs. Besides that, we introduce some new results. The construction of some diffusion operators to embrace numerous higher-order interactions is a pivotal step forwards in this work. Moreover, we incorporate some abstract and real-world numerical illustrations to reinforce our theoretical results.

keywords—Hypergraph, Dynamical network, Dynamical systems, Synchronization, Matrices related to hypergraph, Combinatorics, Applied mathematics

AMS subject classifications— 34D06, 34D20, 05C65, 05C50, 05C90, 05C82.

1. INTRODUCTION

During the last decade, growing interest in studying dynamical networks has been witnessed because of its wide range of applications in some crucial areas of multidisciplinary research involving Chemistry, Computer science, Physics, Mathematics, Biology, Social science, and Information science [1, 2, 6, 8, 11, 14, 18, 21, 33, 43, 45]. The study of the dynamical network deals with the evolution of individual dynamical systems taking place on the vertices of the underlying graph and the consequences of the interactions among the dynamical systems in the different vertices of the graph. This study involves many fundamental concepts from non-linear dynamics and spectral graph theory. The conventional graph topology perspective often can not depict many multi-body interplays in the real world and thus emphasize the need for more sophisticated tools [35, 36]. As an example, to model collaborations among three scientists with a graph, where scientists are considered as vertices and two of them are connected by an edge if they are involved in a project, if we consider a complete graph on three vertices it fails to distinguish between the case where we have one single project, pursued by all the three scientists together or whether there are three different projects pursued by two scientists each. A similar problem arises to represent group formation among the people in social networking platforms like Facebook, WhatsApp, etc [34]. A conceivable treatment of this drawback is implementing hypergraph as the underlying topology of the dynamical network. A hypergraph is a generalization of a graph where the edges are nonempty subsets of the vertex set. A hypergraph is called *(m-) uniform hypergraph*, if each of its edges contains the same (m) , number of vertices, otherwise it is known as general hypergraph (or simply hypergraph). In many real-world interacting systems, the interactions are not pair wise but involve a larger number of vertices at a time [7]. These systems are thus better described using hypergraphs as it's underlying topology. Keeping this type of multi-nary interaction in mind, it is natural to think about the interactions beyond binary. Hyperedges are potential candidates for being a convenient representative of multi-body interactions. We hereby propose a new class of dynamical networks, which is flexible enough to model both the interactions involving two-agents at a time and more than two-agents at a time. In the traditional paradigm, the edges of a graph can incorporate the interactions involving only two agents at a time. Accordingly, in literature, most of the dynamical network models are either represent binary interaction or approximate multi-nary interactions by binary interactions. In contrast, our proposed dynamical network with its hypergraph topology can depict interactions involving any number (≥ 2) of agents.

Synchronization, one of the widely studied phenomena in dynamical systems and networks, was discovered in the year 1665 by Huyghens [15, 44]. According to etymology, the word "Synchronization" has a Greek root "synkhronizein", that means "to occur at the same time", however, in science "synchronization" indicates the

E-mail address: anirban.banerjee@iiserkol.ac.in, samironparui@gmail.com.

Date: December 22, 2024.

coherence of the rhythm of more than one processes. Of late, the field received more observance because of its numerous applications ranging from information spreading to neural networks and rigorous study has been done on different aspects of synchronization in both continuous-time and discrete-time dynamical networks [3, 13, 19, 25–27, 31, 37].

Though a large number of studies have been done on synchronizations of the trajectories of a dynamical network with graph topology, only a few significant contributions have been made so far on the same for dynamical systems on hypergraphs. Before further discussing synchronization in dynamical networks with higher-order interactions, we would like to elucidate some terminology-related ambiguity. In [42], authors have studied synchronization on hyper-network, which is a combination of two or more graphs or simply, multi-layer networks. For more details and references on multi-layer and multiplex networks, readers can see [16, 39]. In literature, sometimes, multi-layer networks and multiplex networks are called hyper-network [42]. The underlying structure of multi-layer networks and multiplex networks are graphs or combinations of graphs, and should not be confused with hypergraphs. Throughout this article, we consider hypergraphs, a generalization of graphs, where each hyperedge can be any subset of the vertex set containing at least two elements. In 2014, the first attempt was made to analyze synchronization in dynamical systems on hypergraphs in which the authors have used continuous-time dynamical systems and analyzed local synchronization with 3-uniform hypergraphs [46]. Very recently a study has been made on local stability analysis of un-weighted continuous-time dynamical systems on hypergraphs in [32]. The diffusion matrix used here is different from ours.

Here, we study local and global synchronization in both, discrete-time and continuous-time dynamical systems on general hypergraphs as well as uniform hypergraphs. The required tools and techniques are developed to generalize the underlying structure of dynamical networks from graphs to hypergraphs. The Laplacian matrices associated with graphs are regarded as convenient tools for describing the diffusive action on the graphs. Later after the advent of the concepts of hypergraphs, the past decades have witnessed many attempts to develop Laplacians for hypergraphs. In this article, some linear operators (and corresponding matrices) are developed to represent the diffusive influence of hyperedges of the hypergraphs. In Section 2 we start with some preliminaries. The main results of this article are given in Section 3. Discrete dynamical systems on hypergraphs is discussed in Section 3.1. In this section, the models for discrete dynamical systems on hypergraphs are proposed and some results involving sufficient conditions on local and global synchronization are derived. A model on weighted discrete dynamical systems on hypergraphs involving variable coupling strength is proposed in Section 3.2 and some results related to global analysis and stability analysis have been stated. Few relations between the structural property of a hypergraph and synchronizability have been discussed in Section 3.3. The continuous-time dynamical systems on hypergraphs is discussed in Section 3.4. As graphs are special cases of hypergraphs, many dynamical networks (with underlying graph architectures) are special cases of our proposed model of coupled dynamical systems on hypergraphs. Thus, some of the results on those special cases are also true for our proposed general case.

In Section 4 and Section 5.2, comparative discussions are given to illustrate the acceptability of hypergraph-architecture over graph-architecture to represent diffusive interaction in multibody framework. We also compute some numerical and real-world examples which are shown in Section 5. All the numerical examples are calculated by using **MATLAB Online R2020a**.

2. PRELIMINARIES

In this section, we introduce and recall some essential and basic definitions and concepts. We start with the notations, that we are going to use throughout this article.

2.1. Notations.

- $\mathbb{N}_k := \{x \in \mathbb{N} : x \leq k, k \in \mathbb{N}\}$.
- We denote a hypergraph by $G = (V, E)$ where V and E are the sets of vertices and (hyper)edges respectively of G . As a graph is a special case of a hypergraph we also use the same notation for graphs. Whether G is a graph or hypergraph that will be cleared from the context. If two distinct vertices, v_i and v_j are connected by an (hyper)edge then we write, $v_i \sim v_j$.
- $m_{max} = \max\{|e_i| : e_i \in E\}$ is the maximum cardinality of the edges, $rank(G)$, of the hypergraph $G = (V, E)$.
- We use the cursive script to denote the tensors and the general script for the matrices. For example, \mathcal{A}_G and \mathcal{L}_G denoted as the adjacency and Laplacian tensors of the hypergraph G , respectively, whereas, A_G and L_G are the adjacency and Laplacian matrices of the G , respectively.
- Here we have considered that the state space of the dynamical systems on each vertex is \mathbb{R}^k . The state of the coupled dynamical systems on hypergraphs at time n is a quantity that represents the situation of the dynamical systems on all the vertices on hypergraphs at time n . Therefore, the state of the coupled dynamical systems on the hypergraph, u is a function $u : TD \times V \rightarrow \mathbb{R}^k$, where TD is the domain of time. For any time $n \in TD$, the state of the coupled dynamical systems on a hypergraph at time n is a function $u(n) : V \rightarrow \mathbb{R}^k$. Thus the state space of the coupled dynamical systems on hypergraphs is

\mathbb{R}^{kV} , the set of all function from V to \mathbb{R}^k . As we consider the cardinality of the vertex set V is equal to N , the state space of the coupled dynamical systems on hypergraphs becomes $\mathbb{R}^{kV} = \mathbb{R}^{Nk}$. The state of the coupled dynamical systems on hypergraphs, with N vertices, at time n is denoted by $u(n)$, a vector in \mathbb{R}^{Nk} . In this article, most of the time the state vector $u(n)$ is represented by an $N \times k$ matrix, whose N rows represent the k dimensional state of the N vertices. However, $u(n)$ can be represented as a kN dimensional vector, we also use the same. Later we will discuss this vector notation. Unless otherwise stated, $u(n)$ is in matrix notation.

- The time is denoted by n and t when we consider the discrete and the continuous cases, respectively.
- $\{u(n)\}_{n \in \mathbb{N}}$ or $\{u(n)\}$ ($\{u(t)\}$ in continuous case) represents the trajectory of a dynamical systems on hypergraphs. In case of matrix notation, $u(n)(i)$ is the i -th row of $u(n)$.
- Synchronized trajectories are of our special interest, thus different notation has been used for this type of trajectories. A synchronized trajectory is denoted by $\{v(n)\}$ (or by $\{v(t)\}$ in continuous case).
- For any symmetric matrices A, B , throughout this paper the following notations are used. $A > 0$ means A is positive definite. $A \geq 0$ means A is positive semidefinite. $A < 0$ means A is negative definite. $A \leq 0$ means A is negative semidefinite. $A > B$ means $A - B$ is positive definite and $A \geq B$ means $A - B$ is positive semidefinite.
- We denote I_k to an identity matrix of order k where $k \in \mathbb{N}$.
- $avg_x(e) := (\sum_{v \in e} x(v))/|e|$ for a hyperedge e and $x \in (\mathbb{R}^k)^V$. Here $|e|$ is the cardinality of e .
- $\mathbf{1}$ is the column vector in \mathbb{R}^N whose all the N components are equal to 1.

2.2. Basic definitions. Before going to define a hypergraph, let us recall the definition of a graph. The order pair, $G = (V, E)$ is called a *graph* where the set V is the collection of vertices and E is a collection of two-element subsets of V , which are called edges. The underlying topology of a conventional dynamical network is a graph. One of the main objectives of this paper to provide a general framework in which hypergraph can be used as the underlying topology of dynamical networks. Replacing graphs by hypergraphs provides the scope of representing multi-nary interactions rather than only binary interactions through the 2-graphs. We refer this generalization of dynamical networks as coupled dynamical systems on hypergraphs. A *hypergraph*, $G = (V, E)$, is a generalized notion of a graph, where a (hyper)edge $e \in E$ can be any nonempty subset (containing at least two elements) of the vertex set, V . In this article, our study is based on finite connected hypergraphs, that is, the vertex sets of the respective hypergraphs are finite. A hypergraph $G(V, E)$ is connected if for any two vertices $v_1, v_l \in V$, there exists a sequence of vertices $v_1 v_2 \dots v_l$, such that, $v_i \sim v_{i+1}$, $i = 1, \dots, l-1$. Throughout the paper, it is considered that the cardinality of vertex set, $|V| = N$ and that of the edge set, $|E| = M$.

As we can represent a graph by different connectivity matrices, such as adjacency matrix, Laplacian matrix, signless Laplacian matrix, normalized Laplacian matrix, etc., analogously a hypergraph can be represented by adjacency tensor, Laplacian tensor, signless Laplacian tensor, normalized Laplacian tensor, etc. Now we recall some definitions of the tensors as described in [5].

Definition 2.1. Let $G = (V, E)$ be the hypergraph with the vertex set $V = \{v_1, v_2, \dots, v_N\}$ and $E = \{e_1, e_2, \dots, e_M\}$. Let m_{max} be the rank(G), of G . The adjacency hyper-matrix of G is defined as the m_{max} order N dimensional tensor $\mathcal{A}_G = \{(a_{i_1 i_2 \dots i_{m_{max}}})\}_{i_j \in \mathbb{N}_N}$. For all edges $e = \{v_{i_1}, v_{i_2}, \dots, v_{i_s}\} \in E$ of cardinality $s \leq m_{max}$, defined by $a_{p_1 p_2 \dots p_{m_{max}}} = \frac{s}{\alpha}$, where $\alpha = \sum_{\substack{k_1, k_2, \dots, k_s \geq 1 \\ \sum_{j \in \mathbb{N}_s} k_j = m_{max}}} \frac{m_{max}!}{k_1! k_2! \dots k_s!}$, where $p_1, p_2, \dots, p_{m_{max}}$ are chosen

from $\{l_1, l_2, \dots, l_s\}$ in all possible ways with at least once for each element of the set. The other positions of the hyper-matrix are zero.

The degree, $d(v)$, of a vertex $v \in V$, is defined by the cardinality of the set $\{e \in E : v \in e\}$. The hypermatrix $\mathcal{D}_G = \{(d_{i_1 i_2 \dots i_{m_{max}}})\}_{i_j \in \mathbb{N}_N}$ of G is the m_{max} order n dimensional diagonal hypermatrix with the entries $d_{ii \dots i} = d(v_i)$ and others are zero.

Definition 2.2. Laplacian hyper-matrix, $\mathcal{L}_G = \{(l_{i_1 i_2 \dots i_{m_{max}}})\}_{i_j \in \mathbb{N}_N}$ of the hyper graph G is the m_{max} order n dimensional diagonal hyper-matrix which is defined as, $\mathcal{L}_G = \mathcal{D}_G - \mathcal{A}_G$

Adjacency, Laplacian, and normalized Laplacian matrices, respectively, for hypergraphs, are introduced in [4]. The operators due to these matrices are linear. Therefore, despite the possibility of losing some information, using these matrices can make our analysis easier because the classical methods of studying synchronization in dynamical networks, which involves linearity of the matrices can be used with some required modification. Now let us recall some definitions of the matrices from [4], to characterize a hypergraph.

Definition 2.3 (Adjacency matrix of hypergraphs). The adjacency matrix $A_G = [(A_G)_{ij}]$ of a hypergraph $G = (V, E)$ is defined as $(A_G)_{ij} = \sum_{e \in E; i, j \in e} \frac{1}{|e|-1}$ if $i \sim j$, and elsewhere it is equal to 0.

Definition 2.4 (Laplacian matrix for hypergraph). *The Laplacian matrix L_G of a hypergraph $G(V, E)$ on n vertices is defined as, $L_G = D_G - A_G$, where D_G is the diagonal matrix where the entries are the degrees $d(i)$ of the i -th vertex of G . Thus,*

$$(L_G)_{ij} = \begin{cases} d(i) & \text{if } i = j, \\ \sum_{\substack{e \in E \\ i, j \in e}} \frac{-1}{|e|-1} & \text{if } i \sim j, \\ 0 & \text{elsewhere.} \end{cases}$$

Definition 2.5. (Normalized Laplacian Matrix) *The normalized Laplacian matrix Δ_G is defined as,*

$$(\Delta_G)_{ij} = \begin{cases} 1 & \text{if } i = j, \\ \frac{1}{d(i)} \sum_{\substack{e \in E \\ i, j \in e}} \frac{-1}{|e|-1} & \text{if } i \sim j, \\ 0 & \text{elsewhere.} \end{cases}$$

A *dynamical system* is a function that describes the evolution of some characteristics (it may be position, quantity, energy, velocity, etc.) of an object with respect to time.

Definition 2.6. *A dynamical system is a function describing the time dependence of the evolution of a variable. If the time is a set of all reals then it is a continuous-time dynamical system (or continuous dynamical system), and if the time is the set of all positive integers, it is called discrete-time dynamical system (or discrete dynamical system).*

The examples of dynamical systems include the motion of a particle, swinging of a pendulum, population of a country in each decade, number of citations of a paper in each year, the bank balance of any bank account at the end of each financial year. In the first two examples, the time is continuous and takes values from non-negative real numbers, and in the other examples, it is a non-negative integer. Therefore the first two are examples of continuous-time dynamical systems, and the other examples are discrete-time dynamical systems.

A *dynamical network* is a graph representing the network with evolving dynamical systems on each of its vertices. The edges of the graph are acting as interconnection or coupling among the dynamical systems in the vertices. If we replace the graph by a hypergraph in the notion of a dynamical network, then we call it *coupled dynamical systems on hypergraph* (CDSH). A CDSH is continuous-time (discrete-time) CDSH if the corresponding dynamical systems in the vertices are continuous (discrete) dynamical systems. Because of the diffusive nature of the couplings, in some cases, the component dynamical systems in all the vertices of the hypergraph may behave similarly after some time (steps). This phenomenon is called *synchronization*.

Definition 2.7. [Synchronization] *A trajectory $\{u(n)\}_{n \in \mathbb{N}}$ of a CDSH with underlying hypergraph G , is said to be synchronized (or synchronous or in sync) if $\lim_{n \rightarrow \infty} \|u(n)(i) - u(n)(j)\| = 0$, for all $i, j \in V(G)$, where $u(n) = (u_{ip}(n))_{i \in \mathbb{N}_N, p \in \mathbb{N}_k} \in \mathbb{R}^{Nk}$ is the state of the CDSH at time n . $(u_{ip}(n))$ denotes the p -th component of the state of the dynamical system on the i -th vertex at time n and the k -component row vector $u(n)(i) \in \mathbb{R}^k$ denotes the state of the dynamics on i -th vertex at time n . The trajectories of a CDSH are called asynchronous if they are not synchronized.*

The manifold, $H = \{(x_{ip})_{i \in \mathbb{N}_N, p \in \mathbb{N}_k} \in \mathbb{R}^{Nk} : x_{1p} = \dots = x_{Np}, \forall p\}$ is called the *manifold of synchronization* of the CDSH. A CDSH synchronizes if its trajectories either fall into the manifold of synchronization after some time or asymptotically converge to the same as time flows. A synchronization is called *global synchronization* if the limit given in Definition 2.7 is 0 for any trajectory, that is independent of any initial conditions, of the CDSH. If a synchronization depends on initial conditions and a trajectory of the CDSH synchronizes, only if it starts from sufficiently close to the manifold of the synchronization, then it is called *local synchronization*.

Now we construct models for CDSH using tensors and matrices associated with hypergraphs and study their synchronizability.

3. COUPLED DYNAMICAL SYSTEMS ON HYPERGRAPHS (CDSH)

In this section, we first look at coupled discrete dynamical systems on hypergraphs. After developing the models, we study local and global synchronizability, respectively, of the trajectories of CDSH represented by the models. After discussing the discrete case on weighted and unweighted multi-body interaction framework we shift to the coupled continuous time dynamical systems on hypergraphs. From now onward unless otherwise stated we consider a CDSH with a hypergraph $G = (V, E)$ as the underlying topology.

3.1. Coupled discrete dynamical systems on hypergraphs. Here we restrict ourselves only in the discrete-time CDSH, and we denote the discrete-time by n . One of the most familiar dynamical network model, that has been reported in the literature [22, 24, 28, 40] for the last few decades is as follows.

$$u(n+1)(i) = \bar{g}(u(n)(i)) + \epsilon \sum_j A_{ij} (\bar{f}(u(n)(j)) - \bar{f}(u(n)(i))), \quad (3.1)$$

where $A = (A_{ij})_{i,j \in \mathbb{N}_N}$ is the adjacency matrix associated with the underlying graph. $\bar{g} : \mathbb{R}^k \rightarrow \mathbb{R}^k$ and $\bar{f} : \mathbb{R}^k \rightarrow \mathbb{R}^k$ are functions governing the dynamics in each vertex i . To introduce the generalized notion for a dynamical network with a hypergraph as its underlying topology, this binary difference term $(\bar{f}(u(n))(j) - \bar{f}(u(n)(i)))$ needs to be replaced with a multi-nary influence corresponding to a hyperedge. To incorporate the multi-nary influence of the hyperedge-coupling corresponding to a hyperedge $e = \{i, j_2, j_3, \dots, j_m\}$ on the dynamical system on the i -th node we introduce the term $\left(\frac{\sum_{j=2}^m \bar{f}(u(n)(j))}{m-1} - \bar{f}(u(n)(i)) \right)$. This term ensures that the action of the hyperedge e influence the dynamics on the i -th vertex to evolve in synchrony with the dynamics on the other vertices that are incident to e . In the beginning, we consider only uniform hypergraphs. Later we extend it to provide a model for non-uniform (general) hypergraphs.

3.1.1. Model for m -uniform hypergraphs. Our coupled discrete dynamical systems on hypergraph model for m -uniform hypergraph is represented as follows.

$$u(n+1)(i) = \bar{g}(u(n)(i)) + \epsilon \sum_{i_2 \dots i_m} a_{ii_2 \dots i_m} \left(\frac{\sum_{j=2}^m \bar{f}(u(n)(i_j))}{m-1} - \bar{f}(u(n)(i)) \right), \quad (3.2)$$

where $\bar{g} : \mathbb{R}^k \rightarrow \mathbb{R}^k$ and $\bar{f} : \mathbb{R}^k \rightarrow \mathbb{R}^k$ are differentiable functions governing the dynamics in each vertex i , $u(n)(i) (\in \mathbb{R}^k)$ is a k -component row vector representing the state of the dynamics in i -th vertex of the systems on hypergraphs at the n -th time step. The p -th component of $u(n)(i)$ is denoted by $(u(n))_{ip} (\in \mathbb{R})$. $\mathcal{A}_G = \{ \{ a_{i_1 i_2 \dots i_m} \}_{i_\alpha \in \mathbb{N}_N} \}_{\alpha \in \mathbb{N}_m}$ and ϵ are the adjacency tensor and the coupling strength, respectively, of the CDSH.

We use the notion of diffusion in this model. Diffusion is the movement of a substance from an area of high concentration to the same of low concentration to make the density uniform, and on the other hand, the hyper-edge couplings of the CDSH are diffusive in nature. Consequently, the interactions through a hyper-edge always try to make the states of all the vertices incident to that hyper-edges equal.

As we mentioned some traditional dynamical networks with graph architecture are a special case of our model, if we put $m = 2$ in Equation (3.2) then it becomes the dynamical network model which has been considered in [22, 24, 28, 40] and moreover, the interaction term that is the second term involving the summation in Equation (3.2) becomes 0 when the synchronization is reached. So, the model represented in Equation (3.2) is a generalization of the dynamical-network models.

For an m -uniform hypergraph we can write the summation on the right side of Equation (3.2) as

$$\begin{aligned} & \sum_{i_2 \dots i_m} a_{ii_2 \dots i_m} \left(\frac{\sum_{j=2}^m \bar{f}(u(n)(i_j))}{m-1} - \bar{f}(u(n)(i)) \right) \\ &= \frac{m}{m-1} \sum_{i_2 \dots i_m} a_{ii_2 \dots i_m} \left(\frac{\sum_{j=2}^m \bar{f}(u(n)(i_j)) + \bar{f}(u(n)(i))}{m} - \bar{f}(u(n)(i)) \right). \end{aligned} \quad (3.3)$$

Thus, if $avg_{f(u(n))}(e_r) = \frac{\sum_{k=2}^m \bar{f}(u(n)(j_k)) + \bar{f}(u(n)(i))}{m}$ is the average of the states of all the vertices associated with the $e_r \in E$ at the n -th time step then the contribution of each $e_r = \{i, j_2, j_3, \dots, j_m\} \in E$ containing the vertex i to the summation in Equation (3.3) is

$$\frac{m}{m-1} (avg_{f(u(n))}(e_r) - \bar{f}(u(n)(i))), \quad (3.4)$$

Since $\sum_{i_2 \dots i_m} a_{ii_2 \dots i_m} = d(i)$, using Equation (3.3) and Equation (3.4), the Equation (3.2) becomes

$$u(n+1)(i) = \bar{g}(u(n)(i)) + \epsilon \frac{m}{m-1} \left[\left(\sum_{e_r \in E(i)} avg_{f(u(n))}(e_r) \right) - d(i) \bar{f}(u(n)(i)) \right] \quad (3.5)$$

So, $u(n+1) = \{u(n+1)(i)\}_{i=1}^N = \{ \bar{g}(u(n)(i)) + \epsilon \frac{m}{m-1} [\left(\sum_{e_r \in E(i)} avg_{f(u(n))}(e_r) \right) - d(i) \bar{f}(u(n)(i))] \}_{i=1}^N$. Here $E(i) = \{e_r \in E : i \in e_r\}$ is the set of all the hyper-edges containing i . Therefore, $|E(i)| = d(i)$ is the degree of the i -th vertex.

3.1.2. Construction of matrices to incorporate diffusive influence of uniform hypergraphs. We now introduce some matrices associated with the underlying hypergraph topology in order to write Equation (3.5) in a more comprehensible and convenient manner. We define the $N \times M$ incidence matrix $\chi_{mG} = \{ \chi_{m_{ir}} \}_{i \in \mathbb{N}_N, r \in \mathbb{N}_M}$ as

$$\chi_{m_{ir}} = \begin{cases} 1 & \text{if } v_i \in e_r \\ 0 & \text{otherwise.} \end{cases} \quad (3.6)$$

It can be easily verified that

$$\frac{1}{m}\chi_{mG}\chi_{mG}^T f(u(n)) = \left\{ \sum_{e_r \in E(i)} avj_{f(u(n))}(e_r) \right\}_{i=1}^N \in \mathbb{R}^{Nk} \quad (3.7)$$

Now suppose that

$$B_m := \left(\frac{1}{m}\chi_{mG}\chi_{mG}^T - D_G \right). \quad (3.8)$$

Using Equation (3.5) and Equation (3.7) we get

$$u(n+1) = g(u(n)) + \epsilon \frac{m}{m-1} B_m f(u(n)), \quad (3.9)$$

From now onwards, we consider Equation (3.9) as the model for CDSH with underlying m -uniform hypergraph-topology, where $u(n) = \{(u(n))_{ip}\}_{i \in \mathbb{N}_N, p \in \mathbb{N}_k} \in \mathbb{R}^{Nk}$ represents the state of the CDSH at time n . Here $(u(n))_{ip}$ is the p -th component of the i -th vertex at time n . The state of the i -th vertex of the CDSH at time n is a k -component vector represented by the i -th row of $u(n)$. The functions $g : \mathbb{R}^{Nk} \rightarrow \mathbb{R}^{Nk}$ and $f : \mathbb{R}^{Nk} \rightarrow \mathbb{R}^{Nk}$ which govern the dynamical systems in all the vertices of the systems on hypergraphs are of special forms, given by $g(\{x_{ip}\}_{i \in \mathbb{N}_N, p \in \mathbb{N}_k}) = (\bar{g}(x_{i1}, x_{i2}, x_{i3}, \dots, x_{ik}))_{i \in \mathbb{N}_N}$ and $f(\{x_{ip}\}_{i \in \mathbb{N}_N, p \in \mathbb{N}_k}) = (\bar{f}(x_{i1}, x_{i2}, x_{i3}, \dots, x_{ik}))_{i \in \mathbb{N}_N}$, respectively. The functions g and f take the above forms as all the vertices are similar, more precisely the dynamics of all the vertices are governed by the same functions \bar{g} and \bar{f} . In matrix notation we write ,

$$f(u(n)) = \begin{pmatrix} \bar{f}(u(n)(1)) \\ \vdots \\ \bar{f}(u(n)(N)) \end{pmatrix} = \begin{pmatrix} \bar{f}_1(u(n)(1)) & \dots & \bar{f}_k(u(n)(1)) \\ \vdots & \ddots & \vdots \\ \bar{f}_1(u(n)(N)) & \dots & \bar{f}_k(u(n)(N)) \end{pmatrix}, \quad (3.10)$$

that is, $f(u(n)) = \{\bar{f}_p(u(n))(i)\}_{i \in \mathbb{N}_N, p \in \mathbb{N}_k}$. Similarly we write $g(u(n)) = \{\bar{g}_p(u(n))(i)\}_{i \in \mathbb{N}_N, p \in \mathbb{N}_k}$.

Remark 3.1. Note that $u(n)$ is a vector in \mathbb{R}^{Nk} and also represented as an $N \times k$ matrix in above. We usually consider $u(n)$ as a matrix, but in some places, we take $u(n)$ as an Nk -dimensional vector whose $((p-1)N+i)$ -th component, which is the state of the p -th components of the dynamical system in i -th vertex, is the (i, p) -th element in its matrix notation. As most of the places we use the matrix notation unless otherwise stated, $u(n)$ is in matrix notation.

Remark 3.2. Now we find some properties of the matrix, B_m . The following result depicts the relevance of B_m as a diffusion operator on an m -uniform hypergraph.

(1) Since

$$x^T B_m x = -\frac{1}{m!} \sum_i \frac{1}{m} \sum_{i_2 \dots i_m} a_{ii_2 \dots i_m} \sum_{j=2}^m (x(i_j) - x(i))^2, \quad (3.11)$$

B_m is negative semi-definite.

- (2) For any connected m -uniform hypergraph and any column vector $x \in \mathbb{R}^N$, $x = c\mathbf{1}$, for some $c \in \mathbb{R}$ if and only if $x^T B_m x = 0$.
- (3) Note that if the underlying hypergraph is connected then any trajectories of the continuous dynamical system $\dot{x} = B_m x$ either fall into the subspace spanned by $\mathbf{1}$ or asymptotically converge to the same. Thus, all the components of the trajectories become equal after some time or their differences become 0 as time flows. The same phenomenon happens with the trajectories of the discrete dynamical system governed by the difference equation $x(n+1) = x(n) + B_m x(n)$, when the operator norm of B_m is less than 2. Thus we consider B_m as a diffusion operator for m -uniform hypergraphs.

Example 3.3. See Example 5.1. All the eigenvalues of B_m are either negative or 0.

3.1.3. *Model for general hypergraphs.* Now we consider the dynamical systems on general hypergraphs, that is, the dynamical networks with general hypergraph as its underlying topology. Thus the model incorporates the interactions among the vertices within the groups (which may have different sizes) simultaneously. First let us define an $N \times M$ matrix $\chi_{mG} = \{\chi_{m_{ir}}\}_{i \in \mathbb{N}_N, r \in \mathbb{N}_M}$ as

$$\chi_{m_{ir}} = \begin{cases} 1 & \text{if } v_i \in e_r, |e_r| = m \\ 0 & \text{otherwise} \end{cases} \quad (3.12)$$

The model for coupled dynamical systems on general hypergraphs is as follows.

$$u(n+1)(i) = \bar{g}(u(n)(i)) + \epsilon \sum_{m=2}^{m_{max}} \frac{m}{m-1} \sum_{e_r \in E(i); |e_r|=m} (avj_{f(u(n))}(e_r) - \bar{f}(u(n)(i))) \quad (3.13)$$

Note that in a hypergraphs there may not exists any edge of cardinality $m \in \mathbb{N}_{m_{max}} - \{1\}$. For that m , the sum, $\sum_{e_r \in E(i); |e_r|=m} (avj_{f(u(n))}(e_r) - \bar{f}(u(n)(i)))$ over a void set is assumed to be zero. suppose that $d^{(m)}(i)$

is the total number of m -edges containing the i -th vertex v_i and diagonal matrix D_{m_G} is defined by $D_{m_G} := \text{diag}(d^{(m)}(i))_{i=1}^N$ and

$$C = \sum_{m=2}^{m_{max}} \frac{m}{m-1} B_m. \quad (3.14)$$

Now we can conclude the following.

$$u(n+1) = \{u(n+1)(i)\}_{i=1}^N = g(u(n)) + \epsilon C f(u(n)), \quad (3.15)$$

Remark 3.4. (1) By Equation (3.14), if the underlying hypergraph is l -uniform then, $C = \frac{l}{l-1} B_l$ and thus, Equation (3.15) becomes Equation (3.9). Consequently, Equation (3.9) is a special case of Equation (3.15).

(2) The matrix C is negative semi-definite.

(3) For any connected hypergraph and any column vector $x \in \mathbb{R}^N$, $x = c\mathbf{1}$, for some $c \in \mathbb{R}$ if and only if $x^T C x = 0$.

Example 3.5. The hypergraph in Example 5.1 is a 9- uniform hypergraph. Thus, here $C = \frac{9}{8} B$.

Example 3.6. All the eigenvalues of C in Example 5.2 are approximately -5.3 , -4.7 , -4.2 , -3.4 , -2.4 , $-8 \times 10^{-16} \approx 0$. and which are non-positive. The same can also be observed in the systems on hypergraphs given in Example 5.6, example 5.4, Example 5.3, Example 5.5 and Example 5.1.

The Remark 3.4.(2) and Remark 3.4.(3) show that all the non-trivial eigenvalues of C are negative. Thus we consider C as a diffusion operator on a connected general hypergraph. We can generalize the model described in Equation (3.15) a little more by introducing an inner coupling matrix Γ , which is a $k \times k$ matrix defined by $\Gamma = (\Gamma_{ij})_{i,j \in \mathbb{N}_k}$ where $\Gamma_{ij} = 1$ if the j -th component of the state on a vertex is effected by the i -th components of the state on the other vertices, otherwise $\Gamma_{ij} = 0$. With Γ , the model becomes

$$u(n+1) = g(u(n)) + \epsilon C f(u(n)) \Gamma = g(u(n)) + \epsilon C T_\Gamma (f(u(n))), \quad (3.16)$$

where $T_\Gamma : \mathbb{R}^{N \times k} \rightarrow \mathbb{R}^{N \times k}$ is a linear operator defined by $T_\Gamma(x) = x\Gamma$, where $x \in \mathbb{R}^{N \times k}$, the set of all real $N \times K$ matrices.

Remark 3.7. Note that $T_\Gamma(Cu(n)) = Cu(n)\Gamma = C T_\Gamma(u(n))$ and thus, the operator norm of T_Γ is $\|T_\Gamma\| = \|\Gamma^T\|$. Therefore, $\|Cu(n)\Gamma\| \leq \|C\| \|u(n)\| \|\Gamma^T\|$.

Now we establish a relation between the matrix C and Laplacian matrix L_G , defined in Definition 2.4.

Theorem 3.8. For any hypergraph G , the matrix $C = -L_G$.

Proof. We know that $C = \sum_{m=2}^{m_{max}} \frac{m}{m-1} B_m = \sum_{m=2}^{m_{max}} \frac{1}{m-1} (\chi_{m_G} \chi_{m_G}^T - D_{m_G}) - \sum_{m=2}^{m_{max}} D_{m_G}$. Therefore, C can be expressed as the following.

$$C = \left(\sum_{m=2}^{m_{max}} \frac{1}{m-1} (\chi_{m_G} \chi_{m_G}^T - D_{m_G}) \right) - D_G. \quad (3.17)$$

For any $k \leq m_{max}$, each row of the matrix I_{k_G} corresponds to a vertex of the hypergraph and each column of I_{k_G} corresponds to a hyper-edge of cardinality k . Thus

$$(\chi_{k_G} \chi_{k_G}^T)_{ij} = \sum_{e_r \in E; |E|=k} (\chi_{k_G})_{ir} (\chi_{k_G})_{rj}^T \quad (3.18)$$

Thus, the contribution of a hyper-edge e_r of cardinality k to $(\chi_{k_G} \chi_{k_G}^T)_{ij}$ is 1 if $v_i, v_j \in e_r$ and 0, otherwise. Thus the same to $(\chi_{k_G} \chi_{k_G}^T)_{ii}$ is 1 if $v_i \in e_r$ and 0 otherwise. Thus we can write

$$(\chi_{k_G} \chi_{k_G}^T)_{ij} = \begin{cases} \sum_{e_r \in E; |E|=k} 1 & \text{if } i \neq j \text{ and } i, j \in e_r \text{ for some } e_r \in E \text{ and } |e_r| = k, \\ d^{(k)}(i) & \text{if } i = j \text{ and } i \in e_r \text{ for some } e_r \in E \text{ and } |e_r| = k, \\ 0 & \text{otherwise.} \end{cases} \quad (3.19)$$

By Equation (3.19) we get the (i, j) -th position of the matrix $\left(\sum_{m=2}^{m_{max}} \frac{1}{m-1} (\chi_{m_G} \chi_{m_G}^T - D_{m_G}) \right)$ is

$$\left(\sum_{m=2}^{m_{max}} \frac{1}{m-1} (\chi_{m_G} \chi_{m_G}^T - D_{m_G}) \right)_{ij} = \begin{cases} \sum_{e \in E} \frac{1}{|e|-1} & \text{if } i, j (\neq i) \in e, \\ 0 & \text{elsewhere.} \end{cases} \quad (3.20)$$

Thus by Definition 2.3, $\sum_{m=2}^{m_{max}} \frac{1}{m-1} (\chi_{m_G} \chi_{m_G}^T - D_{m_G}) = A_G$. Therefore, from Equation (3.17) we have

$$C = A_G - D_G = -L_G. \quad (3.21)$$

□

Now we find sufficient conditions for global and local synchronization. The role of hypergraph-topology in diffusion on the dynamical network can be perceived in terms of a symmetric, zero-row sum matrix. Since our diffusion operators have similarities with existing graph Laplacians, we apply some classical methods and techniques for both, local and global analysis.

3.1.4. *Global synchronization analysis.* suppose that

$$s_1 = \frac{1}{N} \sum_{i=1}^N u(1)(i) (\in \mathbb{R}^k) \quad (3.22)$$

and $v(1)$ is an $N \times k$ matrix whose all the N rows are N copies of s_1 . Consider the trajectory $\{v(n)\}$ of the discrete-time CDSH defined by the Equation (3.16) with the initial state $v(1)$. The iteration rule of $\{v(n)\}$ is as follows.

$$v(n+1) = g(v(n)) + \epsilon C f(v(n)) \Gamma. \quad (3.23)$$

Clearly, because of the equality of its components and the similarity of the dynamics going on each vertex, the trajectory $\{v(n)\}$ is confined in the manifold of synchronization, H . That is all the components of $v(n)$ are the same. Suppose, $v(n)(p) = s_n$ for all $n \in \mathbb{N}$.

Let us define

$$e(n) := u(n) - v(n). \quad (3.24)$$

Thus, Equation (3.16), Equation (3.24), and Equation (3.23) lead us to

$$e(n+1) = g(u(n)) - g(v(n)) + \epsilon C (f(u(n)) - f(v(n))) \Gamma. \quad (3.25)$$

Note that $e(n) \rightarrow 0$ as $n \rightarrow \infty$ manifest the convergence of the trajectory $\{u(n)\}$ to the manifold of synchronization. With this idea we state the following theorem.

Theorem 3.9. *If a CDSH given by Equation (3.16) is such that*

- (1) *f and g are Lipschitz functions with Lipschitz constant k_f and k_g , respectively,*
- (2) *$[k_g + \epsilon \|C\| k_f \|\Gamma^T\|] < 1$, where $\|C\|$ is the operator norm of the matrix C ,*

then any trajectory of the CDSH achieves synchronization asymptotically. Moreover, if $f = g$ and $\Gamma = I$, the identity matrix, then the condition for the synchronization is $\|[I + \epsilon C]\| < \frac{1}{k_f}$.

Proof. By Equation (3.24) and Equation (3.25), $\|e(n+1)\| \leq \|g(u(n)) - g(v(n))\| + \epsilon \|C\| \|f(u(n)) - f(v(n))\| \|\Gamma^T\| \leq (k_g + \epsilon \|C\| k_f \|\Gamma^T\|) \|e(n)\|$. Clearly, if $(k_g + \epsilon \|C\| k_f \|\Gamma^T\|) < 1$, then $e(n) \rightarrow 0$ as $n \rightarrow \infty$. This completes the proof of the first part of the theorem. When, $f = g$ and $\Gamma = I_k$, the Equation (3.25) becomes $e(n+1) = f(u(n)) - f(v(n)) + \epsilon C (f(u(n)) - f(v(n))) = (I + \epsilon C)(f(u(n)) - f(v(n)))$. Therefore, the iteration-rule of the norm of error is $\|e(n+1)\| \leq \|(I + \epsilon C)\| k_f \|e(n)\|$. Thus for $f = g$, if $\|[I + \epsilon C]\| < \frac{1}{k_f}$, then $e(n) \rightarrow 0$ as $n \rightarrow \infty$. This completes the proof. □

The operator norm of a symmetric matrix is the maximum of the absolute values of all the eigenvalues of the matrix. Thus we have the following corollary.

Corollary 3.10. *If the functions f and g are Lipschitz functions with Lipschitz constant k_f and k_g , respectively, and $(k_g + \epsilon \lambda_{max} k_f \|\Gamma^T\|) < 1$, where λ_{max} is the maximum of the absolute values of the eigenvalues of the matrix C , then any trajectory of the CDSH represented by the model in Equation (3.16) achieves synchronization asymptotically. Moreover if $f = g$ and $\Gamma = I$, where I is the identity matrix, then the condition for the synchronization is $\mu_{max} < \frac{1}{k_f}$, where μ_{max} is the maximum of the absolute values of the eigenvalues of $(I + \epsilon C)$.*

Remark 3.11. *Note that in the proof of Theorem 3.9 the condition given in Equation (3.10) have never been used on the functions f and g . Thus, this condition is not needed for the theorem to hold. However, if the functions f and g are such that the condition in Equation (3.10) holds with \bar{f}, \bar{g} and are Lipschitz functions with Lipschitz constants $k_{\bar{f}}$ and $k_{\bar{g}}$, respectively, then f, g are also Lipschitz functions with Lipschitz constants k_f, k_g , respectively, such that $k_f = k_{\bar{f}}, k_g = k_{\bar{g}}$.*

Remark 3.12. *The conditions for synchronization given in Theorem 3.9 and Corollary 3.10 are sufficient conditions, but are not necessary conditions. Thus, sometimes there may be synchronization in the trajectories despite of not complying with the conditions.*

Remark 3.13. *Note that $v(1)$ and s_1 is chosen in such a manner that $v(1)$ depends on $u(1)$ and $v(1) \in H$. This reliance of $v(1)$ on $u(1)$ is just to indicate that $v(1)$ (and therefore, $\{v(n)\}_{n \in \mathbb{N}}$) is not independent from $\{u(n)\}_{n \in \mathbb{N}}$. Thus, there are other choices of s_1 for which $v(1)$ depends on $\{u(n)\}_{n \in \mathbb{N}}$ and $v(1) \in H$. If we consider the projection p of the initial state $u(1)$ on the manifold of synchronization H , then $p = \{p(i)\}_{i \in \mathbb{N}_N} \in H \subset \mathbb{R}^{Nk}$, where $p(i) \in \mathbb{R}^k$. As p is a point on H , all the $p(i)$ are equal and we can choose $s_n = p(i)$ for all $i \in \mathbb{N}_N$. If $f = g$, then instead of considering $s_1 = \frac{1}{N} \sum_{i=1}^N u(1)(i)$, we can take s_1 , as the solution of the uncoupled system $u(n+1)(i) = \bar{f}(u(n)(i))$ (when this solution exists).*

We assumed the existence of synchronized trajectories while proving all the above results on global synchronization. Now we derive some results on global synchronization without any presumption on the existence of the synchronized trajectories and the error terms.

The manifold of synchronization H , defined above, is a k -dimensional subspace of \mathbb{R}^{kN} . Suppose that $\theta(n) = \Lambda u(n)$, where Λ is such a matrix that $\Lambda u(n) = 0$ implies $u(n) \in H$. Therefore, if $\theta(n) \rightarrow 0$ as $n \rightarrow \infty$, then the trajectories of the CDSH converge asymptotically to H and the synchronization is achieved. Thus in order to obtain condition for global synchronization it would be enough to find the condition of $\theta(n) \rightarrow 0$. In order to get the condition for global synchronization that is $\theta(n) \rightarrow 0$ as $n \rightarrow \infty$, we need a recursive relation between $\theta(n+1)$ and $\theta(n)$. If we use the model, given in Equation (3.16) then we have

$$\theta(n+1) = \Lambda u(n+1) \implies \theta(n+1) = \Lambda[g(u(n)) + \epsilon C f(u(n))\Gamma] \quad (3.26)$$

In order to get the recursive relation, on the right side of Equation (3.26) the matrix Λ should have some property to go inside the function g and f in some way, so that we get the term $\Lambda u(n)$. Now we construct a matrix with the desired properties. More precisely, we construct a candidate for being Λ .

Lemma 3.14. *There exists an orthogonal matrix Δ , which commutes with the matrix C . Moreover if the functions f and g are of the form, as described in Equation (3.10) with \bar{f} and \bar{g} are differentiable, and all of their partial derivatives exist and bounded then $\|\Delta f(u(n))\|^2 \leq \|\sup \bar{f}'\|^2 \|\Delta u(n)\|^2$ and $\|\Delta g(u(n))\|^2 \leq \|\sup \bar{g}'\|^2 \|\Delta u(n)\|^2$, where $\|\sup \bar{f}'\|^2 = (\sum_{p \in \mathbb{N}_k} \|\sup(\bar{f}'_p)\|^2)$ and $\|\sup \bar{g}'\|^2 = (\sum_{p \in \mathbb{N}_k} \|\sup(\bar{g}'_p)\|^2)$, $\sup(\bar{f}'_p) = \sup_{q \in \mathbb{N}_k} (\frac{\partial}{\partial x_q} \bar{f}_p(x))$ and $\sup(\bar{g}'_p) = \sup_{q \in \mathbb{N}_k} (\frac{\partial}{\partial x_q} \bar{g}_p(x))$.*

Proof. By Remark 3.4.(2), $-C$ is positive semi-definite. There exists an orthogonal matrix Q such that

$$-C = Q^T D(-C) Q = Q^T (D(-C))^{\frac{1}{2}} Q Q^T (D(-C))^{\frac{1}{2}} Q = \Delta \Delta, \quad (3.27)$$

where $(D(-C))$ is the diagonalization of $-C$ and $\Delta = Q^T (D(-C))^{\frac{1}{2}} Q$ is an orthogonal matrix with the following property,

$$\Delta(-C) = \Delta^3 = (-C)\Delta. \quad (3.28)$$

$$\text{We know } f(u(n)) = \begin{pmatrix} \bar{f}(u(n)(1)) \\ \vdots \\ \bar{f}(u(n))(N) \end{pmatrix} = \begin{pmatrix} \bar{f}_1(u(n)(1)) & \dots & \bar{f}_k(u(n)(1)) \\ \vdots & \ddots & \vdots \\ \bar{f}_1(u(n)(N)) & \dots & \bar{f}_k(u(n)(N)) \end{pmatrix}.$$

We define, $\phi(n)(p) := \Delta \begin{pmatrix} \bar{f}_p(u(n)(1)) \\ \vdots \\ \bar{f}_p(u(n))(N) \end{pmatrix}$. Thus by using Equation (3.14),

$$\begin{aligned} \|\phi(n)(p)\|^2 &= (\phi(n)(p))^T (\phi(n)(p)) \\ &= \sum_{m=2}^{m_{max}} \frac{m}{m-1} \left(\frac{1}{m!} \sum_r \frac{1}{m} \sum_{i_2 \dots i_m} a_{r i_2 \dots i_m} \sum_{j=2}^m (\bar{f}_p(u(n))(i_j) - \bar{f}_p(u(n))(r))^2 \right) \\ &\leq \|\sup(\bar{f}'_p)\| \sum_{m=2}^{m_{max}} \frac{m}{m-1} \frac{1}{m!} \sum_r \frac{1}{m} \sum_{i_2 \dots i_m} a_{r i_2 \dots i_m} \sum_{j=2}^m \|(u(n)(i_j) - u(n)(r))\|^2. \end{aligned} \quad (3.29)$$

As the state of each vertex, $u(n)(i)$ is a k -component vector, we represent $u(n)(i)$ as $\{(u(n)(i))_q\}_{q \in \mathbb{N}_k}$. Thus, $\|(u(n)(i_j) - u(n)(r))\|^2 = \sum_{q=1}^k \|(u(n)(i_j)_q - u(n)(r)_q)\|^2$. Using Equation (3.29) we get

$$\left\| \Delta \begin{pmatrix} \bar{f}_p(u(n)(1)) \\ \vdots \\ \bar{f}_p(u(n))(N) \end{pmatrix} \right\|^2 \leq \sum_{q=1}^k \|\sup(\bar{f}'_p)\|^2 \left\| \Delta \begin{pmatrix} ((u(n)(1))_q) \\ \vdots \\ ((u(n))(N))_q \end{pmatrix} \right\|^2. \quad (3.30)$$

Now after considering the action of Δ on the components of $f(u(n))$ we see the action of Δ on $f(u(n))$. Using Equation (3.30), we get

$$\|\Delta f(u(n))\|^2 \leq \|\sup \bar{f}'\|^2 \|\Delta u(n)\|^2, \quad (3.31)$$

where $\|\sup \bar{f}'\|^2 = (\sum_{p \in \mathbb{N}_k} \|\sup(\bar{f}'_p)\|^2)$.

Since the same result also holds for g , we have

$$\|\Delta g(u(n))\|^2 \leq \|\sup \bar{g}'\|^2 \|\Delta u(n)\|^2, \text{ where } \|\sup \bar{g}'\|^2 = (\sum_{p \in \mathbb{N}_k} \|\sup(\bar{g}'_p)\|^2). \quad (3.32)$$

□

Now we can choose $\Lambda = \Delta$, that is, $\theta(n) = \Delta u(n)$.

Lemma 3.15. *If $\theta(n) = \Delta u(n)$, then $\theta(n) \rightarrow 0$ as $n \rightarrow \infty$ implies that the trajectory $\{u(n)\}_{n \in \mathbb{N}}$ achieves synchronization asymptotically.*

Proof. Expanding the term $\|\Delta u(n)\|^2$ we have,

$$\|\Delta u(n)\|^2 = \sum_{p \in \mathbb{N}_k} \sum_{m=2}^{m_{max}} \frac{m}{m-1} \left[\frac{1}{m!} \sum_i \frac{1}{m} \sum_{i_2 \dots i_m} a_{ii_2 \dots i_m} \sum_{j=2}^m (u(n)(i_j)_p - u(n)(i)_p)^2 \right]. \quad (3.33)$$

Therefore, by Equation (3.33), $\lim_{n \rightarrow \infty} \theta(n) = 0 \implies \lim_{n \rightarrow \infty} \sum_{p \in \mathbb{N}_k} \sum_{m=2}^{m_{max}} \frac{m}{m-1} \left[\frac{1}{m!} \sum_i \frac{1}{m} \sum_{i_2 \dots i_m} a_{ii_2 \dots i_m} \sum_{j=2}^m (u(n)(i_j)_p - u(n)(i)_p)^2 \right] = 0$, that is, $\lim_{n \rightarrow \infty} (u(n)(j)_p - u(n)(i)_p)^2 = 0$ for all $i, j \in \mathbb{N}_N$, and $p \in \mathbb{N}_k$, as the underlying hypergraph is connected. Therefore, result follows. \square

Theorem 3.16. *If the functions f and g are of the form given by Equation (3.10) with \bar{f}, \bar{g} are differentiable functions and $(\|\sup \bar{g}'\| + \epsilon \|\Gamma^T\| \|C\| \|\sup \bar{f}'\|) < 1$, where $\|\sup \bar{f}'\|^2 = (\sum_{p \in \mathbb{N}_k} \|\sup(\bar{f}'_p)\|^2)$ and $\|\sup \bar{g}'\|^2 = (\sum_{p \in \mathbb{N}_k} \|\sup(\bar{g}'_p)\|^2)$, where $\sup(\bar{f}'_p) = \sup_{q \in \mathbb{N}_k} (\frac{\partial}{\partial x_q} \bar{f}_p(x))$ and $\sup(\bar{g}'_p) = \sup_{q \in \mathbb{N}_k} (\frac{\partial}{\partial x_q} \bar{g}_p(x))$, then any trajectory of the CDSH represented by the model in Equation (3.16) achieves synchronization asymptotically.*

Proof. As by Equation (3.28) Δ and C commutes, so to find the sequential trajectory of $\theta(n)$ we consider the recursive relation

$$\theta(n+1) = \Delta u(n+1) = \Delta[g(u(n)) + \epsilon C f(u(n)) \Gamma] = \Delta g(u(n)) + \epsilon C \Delta f(u(n)) \Gamma. \quad (3.34)$$

Therefore, $\|\theta(n+1)\| \leq \|\Delta g(u(n))\| + \epsilon \|C\| \|\Gamma^T\| \|\Delta f(u(n))\| \leq (\|\sup \bar{g}'\| + \epsilon \|C\| \|\Gamma^T\| \|\sup \bar{f}'\|) \|\theta(n)\|$.

Thus, if $(\|\sup \bar{g}'\| + \epsilon \|C\| \|\Gamma^T\| \|\sup \bar{f}'\|) < 1$, then $\theta(n) \rightarrow 0$ as $n \rightarrow \infty$. This completes the proof. \square

If we consider $f = g$ and $\Gamma = I_k$, then the Equation (3.16) becomes

$$u(n+1) = (I_N + \epsilon C) f(u(n)). \quad (3.35)$$

Corollary 3.17. *If the function f is of the form given in Equation (3.10), with \bar{f} is differentiable functions and $\|I_N + \epsilon C\| < \frac{1}{\|\sup \bar{f}'\|}$, where $\|\sup \bar{f}'\|^2 = (\sum_{p \in \mathbb{N}_k} \|\sup(\bar{f}'_p)\|^2)$ and $\|\sup \bar{g}'\|^2 = (\sum_{p \in \mathbb{N}_k} \|\sup(\bar{g}'_p)\|^2)$, where $\sup(\bar{f}'_p) = \sup_{q \in \mathbb{N}_k} (\frac{\partial}{\partial x_q} \bar{f}_p(x))$ and $\sup(\bar{g}'_p) = \sup_{q \in \mathbb{N}_k} (\frac{\partial}{\partial x_q} \bar{g}_p(x))$ then any trajectory of the CDSH represented by Equation (3.35) synchronizes asymptotically.*

Proof. The rule of evolution of the quantity, $\theta(n)$ is $\theta(n+1) = \Delta u(n+1) = \Delta[I_N + \epsilon C] f(u(n)) = [I_N + \epsilon C] \Delta f(u(n))$. Thus, the norm of this quantity must satisfy the following inequality. $\|\theta(n+1)\| \leq \|I_N + \epsilon C\| \|\Delta f(u(n))\| \leq \|I_N + \epsilon C\| \|\sup \bar{f}'\| \|\theta(n)\|$. Thus, the result follows. \square

Remark 3.18. *Note that the condition of synchronization in Corollary 3.17 is not the same with the condition stated in Theorem 3.16. As $\|I_N + \epsilon C\| \leq [1 + \|\epsilon C\|]$, a little different condition of synchronization can be obtained by considering $f = g$ in Theorem 3.16.*

Theorem 3.19. *If f and g are such that $\|f(x)\| \leq k_f \|x\|$, $\|g(x)\| \leq k_g \|x\|$, $\|\Delta(f(x))\| \leq \|f(\Delta x)\|$, $\|\Delta(g(x))\| \leq \|g(\Delta x)\|$, and $(\|k_g\| + \epsilon \|C\| \|k_f\|) < 1$ then any trajectory of CDSH, given by Equation (3.15) achieves synchronization.*

Proof. Using the assumed condition of the theorem we have, $\|\theta(n+1)\| \leq \|g(\Delta u(n))\| + \epsilon \|C\| \|f(\Delta u(n))\| \leq (\|k_g\| + \epsilon \|C\| \|k_f\|) \|\Delta u(n)\| = (\|k_g\| + \epsilon \|C\| \|k_f\|) \|\theta(n)\|$. Therefore, the theorem follows. \square

Remark 3.20. *A natural question is whether such a function f that satisfies all the conditions in Theorem 3.19 exists or not. We try to find the answer in next two examples.*

Example 3.21. *Let F be an $N \times N$ matrix which commutes with Δ (for example F can be any power of Δ) and f is defined by $f(u(n)) = Fu(n)$, where $u(n) = \{(u(n))_{ij}\}_{i \in \mathbb{N}_N, j \in \mathbb{N}_k} (\in \mathbb{R}^{Nk})$ represents the state of the CDSH at time n . Here $(u(n))_{ij}$ is the j -th component of the i -th vertex at time n . As f is linear and $\Delta(f(u(n))) = \Delta Fu(n) = F \Delta u(n) = f(\Delta u(n))$, the function f satisfies the conditions of Theorem 3.19.*

Example 3.22. *If we define $f : \mathbb{R}^{Nk} \rightarrow \mathbb{R}^{Nk}$ as $f = (\bar{f} \ \bar{f} \ \dots \ \bar{f})^T$ where $\bar{f} : \mathbb{R}^k \rightarrow \mathbb{R}^k$ and $\bar{f} = (\bar{f}_i)_{i \in \mathbb{N}_k}$, where $\bar{f}_i : \mathbb{R}^k \rightarrow \mathbb{R}$ and is defined by $\bar{f}_i(x) = \sin(\frac{\pi}{2} \|x\|)$. Here, f is Lipschitz and $\|\Delta f(u)\| = 0 \leq \|f(\Delta u)\|$.*

Before stating the next theorem on global synchronization we prove the following lemma.

Lemma 3.23. *Let R be a symmetric $N \times N$ matrix, whose row sum is 0. If f is a function of the form given in Equation (3.10) such that \bar{f} be a Lipschitz function with $\|\bar{f}(x) - \bar{f}(y)\| \leq k_f \|x - y\|$, then $(f(x))^T R (f(x)) \leq k_f x^T R x$.*

Proof. This result follows from the following steps.

$$\begin{aligned} (f(x))^T R(f(x)) &= (f(x))^T \left(\sum_j R_{ij}(f(x)(j)) \right) \\ &= (f(x))^T \left(\sum_{j \neq i} R_{ij}[(f(x)(j)) - (f(x)(i))] \right) = \sum_{i,j} R_{ij}[(f(x)(j))(f(x)(i)) - (f(x)(i))^2] \\ &\leq k_f^2 \frac{1}{2} \sum_{i,j} R_{ij}[(x(j)) - (x(i))]^2 = k_f^2 x^T R x. \end{aligned} \quad \square$$

Theorem 3.24. *Let R be a negative semi-definite $N \times N$ matrix whose row sum is 0. Let f be a function of the form given in Equation (3.10) such that \bar{f} be a Lipschitz function and $\|\bar{f}(x) - \bar{f}(y)\| \leq k_f \|x - y\|$. If there exists a positive real $b > k_f$ such that $(I_N + \epsilon C)^T R(I_N + \epsilon C) - \frac{1}{b^2} R \geq 0$ then the trajectories of the dynamical system given by Equation (3.35) synchronize.*

Proof. Following Equation (3.27) we claim that there exist a symmetric matrix S such that $R = -S^T S$. If $\alpha(n) = Su(n)$ then $\|\alpha(n+1)\|^2 = (\alpha(n+1))^T (\alpha(n+1)) = (u(n+1))^T S^T Su(n+1) = -(u(n+1))^T Ru(n+1)$. By using Equation (3.35) we get, $-\|\alpha(n+1)\|^2 = (f(u(n)))^T [I_N + \epsilon C]^T R([I_N + \epsilon C]f(u(n))) \geq \frac{1}{b^2} (f(u(n)))^T R f(u(n))$. As R is a symmetric zero-sum matrix, so is $-R$. Consequently, by Lemma 3.23 we have $\|\alpha(n+1)\|^2 \leq k_f^2 \frac{1}{b^2} (u(n))^T (-R)(u(n)) = \left(\frac{k_f}{b}\right)^2 \|\alpha(n)\|^2$. As $k_f < b$, $\alpha(n) = Su(n) \rightarrow 0$, as $n \rightarrow \infty$. Thus, if $\lim_{n \rightarrow \infty} u(n) = u$ then $Su = 0$. Thus, $\|Su\|^2 = 0 \implies (Su)^T (Su) = 0 \implies u^T Ru = 0$. As R is a symmetric matrix which have 0 row sum,

$$u^T Ru = 0 \implies \frac{1}{2} \sum_{ij} R_{ij} (u(i) - u(j))^2 = 0. \quad (3.36)$$

As the underlying hypergraph is connected, from the above Equation (3.36) we have $u(i) = u(j)$, for all $i, j \in \mathbb{N}_N$. This completes the proof. \square

In the above subsection, we state some results with global sufficient conditions for synchronization. We call these conditions global as they are independent of local parameters such as initial conditions, pivot around some global aspects like Lipschitz constants, and the supremum of all the partial derivatives. In the subsequent subsection, we state results involving local parameters.

3.1.5. Local stability analysis. Here we consider the trajectories of the CDSH, which start from neighboring points of the manifold of synchronization.

Before going into local analysis, let us have a bird's-eye view on linearization. Let $h : \mathbb{R}^n \rightarrow \mathbb{R}$ be a smooth function, $a \in \mathbb{R}^n$ be a fixed point and $x \in \mathbb{R}^n$ be any arbitrary point. The Taylor series of $h(x)$ about a is given by,

$$h(x) = h(a) + \frac{1}{i!} \sum_{i \in \mathbb{N}} (\nabla^i f(a))(x - a)^i, \quad (3.37)$$

where $\nabla^i h(a)$ is a i -th order n -dimensional symmetric tensor (for details see [38, example-1.1 in chapter-1]) given by $\nabla^i h(a)_{j_1 j_2 \dots j_i} = \frac{\partial^i (h(a))}{\partial x_{j_1} \partial x_{j_2} \dots \partial x_{j_i}}$. For any m -order n -dimensional tensor $\mathcal{T} = \{\{t_{j_1 \dots j_m}\}_{j_r \in \mathbb{N}_n}\}_{r \in \mathbb{N}_m}$ and $x \in \mathbb{C}^n$, the product $\mathcal{T}x^m$ (as defined in [38, page-4]) is defined as $\mathcal{T}x^m = \mathcal{T} \times_1 x \times_2 x \times_3 \dots \times_m x = \sum_{j_1, j_2, \dots, j_m \in \mathbb{N}_n} t_{j_1 j_2 \dots j_m} x(j_1) x(j_2) \dots x(j_m)$. For $i = 1$, $\nabla^i h(a)$ is called the gradient of h at a and for $i = 2$ it is the Hessian matrix of h evaluated at a .

Now if x is sufficiently neighboring to a , that is, x is in a sufficiently small neighbourhood of a then $(x - a)$ is very small in modulus. The nonlinear terms in Equation (3.37) involving the powers of $(x - a)$ become very small and thus, the truncated linear part of the right hand side of Equation (3.37) can be treated as a good approximation of $h(x)$ for any x sufficiently adjacent to a . This approximation is called the linearization of h around a . Thus, in a precise form, the linearization of h around a is given by

$$h(x) = h(a) + (\nabla h(a))(x - a). \quad (3.38)$$

Expanding it we get, $h(x) = h(a) + \sum_{i \in \mathbb{N}_n} (x - a)_i \frac{\partial h(a)}{\partial x_i}$. Note that, if we consider x and a as row vectors

then we can assume $Dh(a) = \left\{ \frac{\partial h(a)}{\partial x^i} \right\}$ as a column vector. In that case Equation (3.38) can be rewritten as $h(x) = h(a) + (x - a) \cdot Dh(a)$ If we consider x and a are column vectors, respectively and $Dh(a) = \left\{ \frac{\partial h(a)}{\partial x^i} \right\}$ is a row vector, Equation (3.38) becomes $h(x) = h(a) + Dh(a) \cdot (x - a)$. Now we are in a position to consider the stability analysis of synchronization.

Lemma 3.25. *The stability of synchronization of a synchronized trajectory and the local synchronizability of a trajectory which started very near to the manifold of synchronization of the CDSH, given by Equation (3.16) depends on the local stability of a dynamical system around 0.*

Proof. suppose that $u(1) \in \mathbb{R}^{Nk}$ be a point, very close to the manifold of synchronization, H . That is, there exists a point $v(1) \in H \subset \mathbb{R}^{Nk}$ such that $e(1) = u(1) - v(1)$ and $\|e(1)\|$ are sufficiently small. Let $\{u(n)\}_{n \in \mathbb{N}}$ and $\{v(n)\}_{n \in \mathbb{N}}$ be two trajectories of the discrete CDSH represented by Equation (3.16) with initial points $u(1)$ and $v(1)$, respectively and $\{e(n)\}_{n \in \mathbb{N}}$ is the trajectory defined by $e(n) = u(n) - v(n)$. Using Equation (3.16) we have,

$$\begin{aligned} e(n+1) &= (g(u(n)) + \epsilon C f(u(n))\Gamma) - (g(v(n)) + \epsilon C f(v(n))\Gamma) \\ &= g(u(n)) - g(v(n)) + \epsilon C (f(u(n)) - f(v(n)))\Gamma \end{aligned} \quad (3.39)$$

By Equation (3.16), $v(1) \in H \implies v(n) \in H$ for all $n \in \mathbb{N}$. If $e(n) \rightarrow 0$, as $n \rightarrow \infty$, then the local synchronization is achieved by the trajectory $\{u(n)\}_{n \in \mathbb{N}}$ and the synchronization of the synchronized trajectory $\{v(n)\}_{n \in \mathbb{N}}$ is stable under any small perturbation. Our next aim is to find the equation governing the trajectory $\{e(n)\}_{n \in \mathbb{N}}$ of the error dynamical system using Equation (3.39) and analyse its stability around 0.

Now using Equation (3.10) we have,

$$\begin{aligned} f(u(n)) &= \begin{pmatrix} \bar{f}_1(v(n)(1)) & \dots & \bar{f}_k(v(n)(1)) \\ \vdots & \ddots & \vdots \\ \bar{f}_1(v(n)(N)) & \dots & \bar{f}_k(v(n)(N)) \end{pmatrix} \\ &+ \begin{pmatrix} (e(n)(1)).D\bar{f}_1(v(n)(1)) & \dots & (e(n)(1)).D\bar{f}_k(v(n)(1)) \\ (e(n)(N)).D\bar{f}_1(v(n)(N)) & \dots & (e(n)(N)).D\bar{f}_k(v(n)(N)) \end{pmatrix}. \end{aligned} \quad (3.40)$$

As we know $v(n) \in H$, for all $n \in \mathbb{N}$, $v(n)(1) = v(n)(2) = \dots = v(n)(N) = s_n \in \mathbb{R}^k$ and thus, we rewrite Equation (3.40) as

$$f(u(n)) = f(v(n)) + e(n).J_f(n), \quad (3.41)$$

where $e(n) = (e(n)(1) \ e(n)(2) \ \dots \ e(n)(N))^T$ is an $N \times k$ matrix and $J_f(n) = (D\bar{f}_1(s_n) \ \dots \ D\bar{f}_k(s_n))$ is a $k \times k$ matrix. Similarly, for the function g , we get

$$g(u(n)) = g(v(n)) + e(n).J_g(n). \quad (3.42)$$

Therefore, by using Equation (3.41) and Equation (3.39) we have,

$$e(n+1) = e(n)J_g(n) + \epsilon C e(n)J_f(n)\Gamma. \quad (3.43)$$

Clearly the condition for the stability of the synchronized trajectory $\{v(n)\}_{n \in \mathbb{N}}$ and the condition for the local synchronization of $\{u(n)\}_{n \in \mathbb{N}}$ is the condition for the local stability of the error system represented in Equation (3.43).

As, C is a symmetric matrix, there exists an orthogonal matrix Q (the rows of Q are the eigenvectors of C) such that $C = Q^T D_C Q$, where D_C is the diagonalization of C . Now from Equation (3.43) we get, $Qe(n+1) = Qe(n)J_g(n) + \epsilon Q C Q^T Qe(n)J_f(n)\Gamma$. Thus, it can be concluded that

$$\eta(n+1) = \eta(n)J_g(n) + \epsilon D_C \eta(n)J_f(n)\Gamma, \quad (3.44)$$

where $\eta(n) = Qe(n)$ for all $n \in \mathbb{N}$. Thus, $\eta(n+1)(i) = \eta(n)(i)(J_g(n) + \epsilon \lambda_i J_f(n)\Gamma)$. Therefore,

$$\eta(n+1)(i) = \left\{ \prod_{k=1}^n (J_g(k) + \epsilon \lambda_i J_f(k)\Gamma) \right\} \eta(1)(i), \quad (3.45)$$

for all $i \in \mathbb{N}_N$. Here $\{\lambda_i\}_{i \in \mathbb{N}_N}$ are all the eigenvalues of C . Clearly, as $n \rightarrow \infty$, if $\eta(n) \rightarrow 0$ then $e(n) \rightarrow 0$. Thus, the condition for local synchronization of $\{u(n)\}_{n \in \mathbb{N}}$ and the condition for stability of the synchronization of $\{v(n)\}_{n \in \mathbb{N}}$ are the conditions for stability of $\{\eta(n)_i\}_i$ for all $i \in \mathbb{N}_N$ around the equilibrium point 0. \square

Now we construct a Lyapunov function for local synchronization. Let A be a positive definite $k \times k$ matrix. Let $V : \mathbb{R}^N \rightarrow \mathbb{R}$ be a function defined by

$$V(x) = xAx^T. \quad (3.46)$$

Clearly, $V(x) \geq 0$ for all row vector $x \in \mathbb{R}^n$. Now we have

$$V(\eta(n+1)_i) = (\eta(n)(i)(J_g(n) + \epsilon \lambda_i J_f(n)\Gamma))A(\eta(n)(i)(J_g(n) + \epsilon \lambda_i J_f(n)\Gamma))^T \quad (3.47)$$

Note that the notion of the stability of synchronization of the synced trajectory $\{v(n)\}$ and the same of local synchronization of any trajectory $\{u(n)\}$ are like two peas in a pod. Thus the study on any one of the two notions suffices for the other too. As A is positive definite, we can write $V(x) = \|x\|_A$, where $\|\cdot\|_A$ is a norm on \mathbb{R}^N . Now we are in position to state and prove the following results on local synchronization.

Lemma 3.26. *The synchronization of the synced trajectory $\{v(n)\}_{n \in \mathbb{N}}$ of CDSH given by Equation (3.16) is stable under a small perturbation if and only if $\|(J_g(n) + \epsilon \lambda_i J_f(n)\Gamma)\|_A < 1$.*

Proof. Writing Equation (3.47) in with the notation of $\|\cdot\|_A$ we have

$$\|\eta(n+1)(i)\|_A = \|(\eta(n)(i)\|_A \|(J_g(n) + \epsilon\lambda_i J_f(n)\Gamma)\|_A)\|_A, \quad (3.48)$$

which implies $\eta(n)$ is stable around 0 if and only if $\|(J_g(n) + \epsilon\lambda_i J_f(n)\Gamma)\|_A < 1$ for all $i \in \mathbb{N}_N$. Thus, by using Lemma 3.25, we get our desired result. \square

Theorem 3.27. *Let the limit, $\sigma = \lim_{n \rightarrow \infty} \frac{1}{n} \sum_{r=1}^n \log \|J_f(r)\|_A$ exists and $f = g$ and $\Gamma = c.I_k$, for some constant c . The synchronization of the synced trajectory $\{v(n)\}_{n \in \mathbb{N}}$ of CDSH given by Equation (3.16) is stable under a small perturbation if all the absolute values of the eigenvalues of C are contained in the interval $[\frac{1-e^{-\sigma}}{c\epsilon}, \frac{1+e^{-\sigma}}{c\epsilon}]$.*

Proof. As $f = g$, and $\Gamma = c.I_k$ Equation (3.48) becomes $\|\eta(n+1)(i)\|_A \leq \|(\eta(n)(i)\|_A \|(1 + \epsilon c\lambda_i)\|)\|_A \|J_f(n)\|_A$. Thus, we have,

$$\|\eta(n+1)(i)\|_A = \|(\eta(1)(i)\|_A \|(1 + \epsilon c\lambda_i)\|)^n \left(\prod_{r=1}^n \|J_f(r)\|_A \right), \quad (3.49)$$

which implies $\eta(n) \rightarrow 0$ as $n \rightarrow \infty$, if $\|(1 + \epsilon c\lambda_i)\| \left(\prod_{r=1}^n \|J_f(r)\|_A \right)^{\frac{1}{n}} < 1$, for all i , that is equivalent to

$$\|(1 + \epsilon c\lambda_i)\| e^\sigma < 1, \quad (3.50)$$

for all i , where $\sigma = \lim_{n \rightarrow \infty} \log \left(\left(\prod_{r=1}^n \|J_f(r)\|_A \right)^{\frac{1}{n}} \right) = \lim_{n \rightarrow \infty} \frac{1}{n} \sum_{r=1}^n \log \|J_f(r)\|_A$. Therefore, the trajectories of the

CDSH represented by Equation (3.16), synchronize locally if $\frac{1-e^{-\sigma}}{c\epsilon} < -\lambda_i < \frac{1+e^{-\sigma}}{c\epsilon}$ for all $i = 1, 2, \dots, N$. In other words, the synchronization is stable under small perturbation if the above condition satisfied. This completes the proof. \square

In fact from Lemma 3.26, we can conclude a little more than Theorem 3.27 but before that we need the following remark.

Remark 3.28. *The rows of Q are the eigenvectors of C . Thus, the eigenvalues of C has one to one correspondence with the rows of Q . As the r -th row $Qe(1)$ is obtained by right multiplication of $e(1)$ with the r -th row of Q (that is with the transpose of an eigenvector of C), the r -th row of $Qe(1)$ also has an one to one correspondence with the eigenvalues of C . That is if λ_r is the r -th eigenvalue with eigenvector v_r then r -th row of Q is $Q_r = v_r$ and the r -th row of $Qe(1)$ is $v_r^T e(1)$. We are going to use this correspondence in the next result.*

Theorem 3.29. *Let the limit, $\sigma = \lim_{n \rightarrow \infty} \frac{1}{n} \sum_{r=1}^n \log \|J_f(r)\|_A$ exists and $f = g$, $\Gamma = c.I_k$, for some constant $c > 0$. Let $e(1)$ be the initial perturbation of synchronized trajectory. The synchronization of the synced trajectory $\{v(n)\}_{n \in \mathbb{N}}$ of CDSH given by Equation (3.16) is stable under a small perturbation if and only if either the i -th row (component) of the $Qe(1) = \eta(1)$ is zero or the absolute value of the corresponding i -th eigenvalue of C is contained in the interval $[\frac{1-e^{-\sigma}}{c\epsilon}, \frac{1+e^{-\sigma}}{c\epsilon}]$.*

Proof. From Equation (3.49), it can be concluded that $\lim_{n \rightarrow \infty} \eta(n)(i) = 0$ if and only if either $\eta(1)(i) = 0$ or $\|(1 + \epsilon c\lambda_i)\| e^\sigma < 1$. Using this fact and proceeding like the proof of Theorem 3.27, this result can be proved easily. \square

Remark 3.30. *The rows of Q are the eigenvectors of C . Let the r -th row of Q (say Q_r) is the eigenvector of C corresponding to the eigenvalue 0. So $Q_r \in \mathbb{R}^N$ with all its components are equal to 1. If we choose s_1 as defined in Equation (3.22) and $V(1)$ accordingly (that is, if we do not choose the other options for s_1 given in Remark 3.13), then the r -th component of $\eta(1) (= Qe(1))$ can be written, by using Equation (3.22), as $Q_r \cdot e(1) = Q_r \cdot (u(1) - v(1)) = \sum_{i \in \mathbb{N}_N} u(1)(i) - \sum_{i \in \mathbb{N}_N} v(1)(i) = 0$. Thus, by Theorem 3.29, we have the following result.*

Corollary 3.31. *Let the limit, $\sigma = \lim_{n \rightarrow \infty} \frac{1}{n} \sum_{r=1}^n \log \|J_f(r)\|_A$ exists and $f = g$, $\Gamma = c.I_k$, for some constant $c > 0$. The synchronization of the synced trajectory $\{v(n)\}_{n \in \mathbb{N}}$ of CDSH given by Equation (3.16) is stable under a small perturbation if all the absolute values of the nonzero eigenvalues of C are contained in the interval $[\frac{1-e^{-\sigma}}{c\epsilon}, \frac{1+e^{-\sigma}}{c\epsilon}]$.*

Proof. This result directly follows from Remark 3.30 and Theorem 3.29. \square

The next corollary easily follows from Theorem 3.27, Remark 3.30.

Corollary 3.32. *If $f = g$, $\Gamma = c.I_k$ for some constant $c > 0$, the limit $\sigma = \lim_{n \rightarrow \infty} \frac{1}{n} \sum_{r=1}^n \log \|J_f(r)\|_A$ exists, and the coupling strength ϵ is contained in the interval $[\frac{1-e^{-\sigma}}{c\lambda_{\min}}, \frac{1+e^{-\sigma}}{c\lambda_{\max}}]$, where λ_{\max} and λ_{\min} are the maximum and minimum of the absolute values of the nonzero eigenvalues of C respectively then the synchronization of the synchronized trajectory $\{v(n)\}_{n \in \mathbb{N}}$ of the CDSH, given by Equation (3.16) is stable under small perturbation.*

Proof. If $\epsilon \in [\frac{1-e^{-\sigma}}{c\lambda_{\min}}, \frac{1+e^{-\sigma}}{c\lambda_{\max}}]$ where λ_{\max} and λ_{\min} are the maximum and minimum of the absolute values of the non zero eigenvalues of C respectively, then $\frac{1-e^{-\sigma}}{c\epsilon} < \lambda_{\min} < \lambda_{\max} < \frac{1+e^{-\sigma}}{c\epsilon}$. Therefore, $\frac{1-e^{-\sigma}}{c\epsilon} < \|\lambda_i\| < \frac{1+e^{-\sigma}}{c\epsilon}$ for all nonzero eigenvalues λ_i of C , that is $\frac{1-e^{-\sigma}}{c\epsilon} < -\lambda_i < \frac{1+e^{-\sigma}}{c\epsilon}$. This can be written as $-e^{-\sigma} < 1 + \epsilon c \lambda_i < e^{-\sigma}$, or in terms of absolute value, $\|(1 + \epsilon c \lambda_i)\| e^\sigma < 1$. Therefore, the result follows from Equation (3.50) and Remark 3.30. \square

Note that in the above results the quantity σ depends on the choice of initial perturbation. Consequently, the results involving σ take into account the local synchronization (or more precisely the stability of synchronization) only. Now we recall some results from [9] and [10].

Lemma 3.33. [10, page-7, equation(2.3),(2.4)] $\begin{pmatrix} Q(x) & S(x) \\ S^T(x) & R(x) \end{pmatrix} > 0$ is equivalent to $R(x) > 0$, $Q(x) - S(x)R(x)^{-1}S(x)^T > 0$, where $Q(x) = Q(x)^T$, $R(x) = R(x)^T$, and $S(x)$ depends affinely on x .

Lemma 3.34. [9, Theorem 1.2 (Existence of a Lyapunov function implies stability), page-2] Let $x = 0$ be an equilibrium point for the autonomous system $x(t+1) = f(x(t))$ where $f : D \rightarrow \mathbb{R}^n$ is locally Lipschitz in $D \subset \mathbb{R}^n$ and $0 \in D$. suppose that there exists a continuous function $V : D \rightarrow \mathbb{R}$ such that $V(0) = 0$ and $V(x) > 0$, for all $x \in D - \{0\}$ and $V(f(x)) - V(x) \leq 0$, for all $x \in D$. Then $x = 0$ is stable. Moreover if $V(f(x)) - V(x) < 0$, for all $x \in D - \{0\}$ then $x = 0$ is asymptotically stable.

Lemma 3.35. [9, Theorem 1.4 (Existence of a Lyapunov function implies stability), page-2] Let $x = 0$ be an equilibrium point for the autonomous system $x(t+1) = f(x(t))$ where $f : D \rightarrow \mathbb{R}^n$ is locally Lipschitz in $D \subset \mathbb{R}^n$ and $0 \in D$. suppose that there exists a continuous function $V : D \rightarrow \mathbb{R}$ such that $V(0) = 0$ and $V(x) > 0$, for all $x \in D - \{0\}$ and $V(x) \rightarrow 0$ as $\|x\| \rightarrow \infty$ and $V(f(x)) - V(x) < 0$, for all $x \in D - \{0\}$ then $x = 0$ is globally asymptotically stable.

Now we have the following theorem.

Theorem 3.36. If there exists a positive definite matrix A such that $[((J_g(n) + \epsilon \lambda_i J_f(n) \Gamma))A((J_g(n) + \epsilon \lambda_i J_f(n) \Gamma))^T - A] < 0$ for all i then local synchronization is achieved by any trajectory $\{u(n)\}_{n \in \mathbb{N}}$ and the synchronization of the synchronized trajectory $\{v(n)\}_{n \in \mathbb{N}}$ of the CDSH given by Equation (3.16) is stable under small perturbation.

Proof. We have,

$$\begin{aligned} V(\eta(n+1)_i) - V(\eta(n)_i) \\ = (\eta(n)_i)[((J_g(n) + \epsilon \lambda_i J_f(n) \Gamma))A((J_g(n) + \epsilon \lambda_i J_f(n) \Gamma))^T - A](\eta(n)_i)^T. \end{aligned} \quad (3.51)$$

Thus, if $[((J_g(n) + \epsilon \lambda_i J_f(n) \Gamma))A((J_g(n) + \epsilon \lambda_i J_f(n) \Gamma))^T - A]$ is negative definite, then $V(\eta(n+1)_i) - V(\eta(n)_i) \leq 0$ and the result follows from Lemma 3.34, Lemma 3.35. \square

Therefore, by using Lemma 3.33, Lemma 3.35 we have the next corollary.

Corollary 3.37. If there exists a positive definite matrix A such that

$$\begin{pmatrix} A & (J_g(n) + \epsilon \lambda_i J_f(n) \Gamma) \\ ((J_g(n) + \epsilon \lambda_i J_f(n) \Gamma))^T & A^{-1} \end{pmatrix} > 0$$

for all i then local synchronization is achieved by any trajectory $\{u(n)\}_{n \in \mathbb{N}}$ and the synchronization of the synchronized trajectory $\{v(n)\}_{n \in \mathbb{N}}$ of the discrete dynamical system given by Equation (3.16) is stable under small perturbation.

Remark 3.38. If we take the maximum edge cardinality, $m_{max} = 2$, all the underlying hypergraphs of the models, discussed above, become graphs and the corresponding CDSH become dynamical networks. Thus, some of the above results on CDSH can be considered as generalization of the same on dynamical-networks found in [22, 24, 29].

3.2. Synchronization in discrete coupled dynamical systems on weighted hypergraphs. Two groups of agents, despite being of the same size, may have different impacts on the overall dynamics in some real-world complex systems. To incorporate this discrepancy among the different interactive groups of agents we introduce weights for hyperedges in this section. Let $G = (V, E, w)$ be a weighted hypergraph with vertex set V , edge set E , and a weight function $w : E \rightarrow \mathbb{R}^+$. The positive real number $w(e)$ is called the weight of the hyper-edge e [41]. One may consider the \mathbb{R} as the range of the weight function, but in this work, we restrict the same to \mathbb{R}^+ .

In a CDSH, the hyper-edges act as the interactive couplings. It is natural to expect a condition of synchronization governed by hyper-edges. Now for each edge $e = (v_{i_1}, v_{i_2}, \dots, v_{i_j})$ with cardinality j , we define a function $h_e : \mathbb{R}^{N^k} \rightarrow \mathbb{R}^{N^k}$ by

$$h_e(u)(i) = \begin{cases} \frac{j}{j-1}(av_{j_u}(e) - u(i)) & \text{if the } i\text{-th vertex } v_i \in e, \\ 0 & \text{otherwise,} \end{cases} \quad (3.52)$$

where $avj_u(e) = \frac{\sum_{r \in \mathbb{N}_j} u(i_r)}{j}$ and $u(i) \in \mathbb{R}^{Nk}$. The function h_e can be considered as action of the edge e on the state of the vertices (or simply, the action of e). Note that an edge e_r has a non-zero action on the vertex v_j only if (v_j, e_r) is an edge in the incidence graph of the systems on hypergraphs.

Now we study the linearity in this action of hyper-edges. We define an $N \times 1$ matrix χ_e and an $N \times N$ diagonal matrix D_e corresponding to a hyper-edge e by, $(\chi_e)_i = 1$ if $v_i \in e$, otherwise $(\chi_e)_i = 0$ and $(D_e)_{ii} = 1$ if $v_i \in e$, otherwise $(D_e)_{ii} = 0$. It can be easily verified that

$$h_e(u) = H_e u, \text{ where } H_e := \frac{|e|}{|e|-1} \left(\frac{1}{|e|} \chi_e \chi_e^T - D_e \right). \quad (3.53)$$

As the action of H_e always tries to make the state of the dynamics on all the vertices associated with e evolve in synchrony and the action vanishes when the state of the dynamics of all the vertices incident to e becomes equal, we call the $N \times N$ symmetric matrix H_e the *edge-diffusion matrix of the edge e* . Now using Equation (3.53) we re-write the general model represented in Equation (3.13) as

$$u(n+1)(i) = \bar{g}(u(n)(i)) + \epsilon \sum_{m=2}^{m_{max}} \frac{m}{m-1} \sum_{e_r \in E(i); |e_r|=m} (avj_{(f(u(n)))}(e_r) - \bar{f}(u(n)(i))) \quad (3.54)$$

that leads us to

$$u(n+1) = \{u(n+1)(i)\}_{i \in \mathbb{N}_N} = g(u(n)) + \epsilon \sum_{e_r \in E} H_{e_r}(f(u(n))) \quad (3.55)$$

Now Equation (3.55) is our model to study the action of edge and its effect on synchronization in discrete CDSH. This model can be generalized further by introducing a $k \times k$ inner couple matrix Γ as follows.

$$u(n+1) = g(u(n)) + \epsilon \sum_{e_r \in E} H_{e_r}(f(u(n)))\Gamma. \quad (3.56)$$

Remark 3.39. *The model represented by Equation (3.15) is equivalent to the model given by Equation (3.55) as both of them are equivalent to the model described in Equation (3.13). Similarly the model in Equation (3.16) is equivalent to the model given by Equation (3.56). It is obvious that any theorem, holds for the trajectories of a CDSH model, will also hold for all its equivalent models.*

In the previous sections, we have considered the coupling strength ϵ as a constant for all couplings. Now we take different coupling strengths for the couplings, i.e., for the hyperedges. So, we consider ϵ as a function. In fact, we define the coupling strength of a hyperedge e as the function of the weight, $w(e)$ of e . suppose that $\alpha_e : \mathbb{R}^+ \rightarrow \mathbb{R}^+$ is a positive real valued function corresponding to a hyperedge $e \in E$. We define $\epsilon : E \rightarrow \mathbb{R}^+$ as $\epsilon(e) = \alpha_e(w(e))$ for all $e \in E$ for our dynamical network with weighted hypergraphs architecture model. One may choose the identity map for all α_e to get the coupling strengths equal to the corresponding edge-weights.

After taking ϵ_e in Equation (3.56) we have the following weighted systems on hypergraphs model.

$$u(n+1) = g(u(n)) + \sum_{e_r \in E} \left\{ \epsilon_{e_r} H_{e_r}(f(u(n)))\Gamma \right\}. \quad (3.57)$$

3.2.1. *Global analysis of coupled discrete dynamical systems on weighted hypergraphs.* Let

$$L_w := \sum_{e_p \in E} \epsilon_{e_p} H_{e_p}. \quad (3.58)$$

Now the Equation (3.57) becomes

$$u(n+1) = g(u(n)) + L_w(f(u(n)))\Gamma. \quad (3.59)$$

Remark 3.40. *We listed below some observations on L_w .*

- (1) L_w is symmetric and negative semidefinite.
 - (2) If G be a weighted hypergraph and w_e be the weight of a hyper-edge e of G . Then $L_w = A_w - \sum_{e \in E} \epsilon_e D_e$.
- Here A_w is the adjacency matrix of a weighted hypergraph considered in [41, section-2].

For Dynamical networks with graph as its underlying architecture, the Laplacian matrix of the underlying graph is used as the diffusion operator ([22, 24, 25, 28, 37, 40] and many more). For dynamical networks with hypergraph as its underlying structure, it is easy to see that 0 is an eigenvalue of L_w , and for a connected hypergraph, the eigenspace of 0 is the one-dimensional vector space generated by $\mathbf{1}$. Therefore, L_w is a reasonable candidate for being a diffusion operator for a weighted non-uniform hypergraph. Evidently, L_w is symmetric and has zero row sum for weighted hypergraphs. Now we find similar results in our study for weighted hypergraphs as we have for unweighted hypergraphs. Thus in many cases, the proofs are also similar and therefore, being omitted with proper references.

Now we define the matrix D_w as follows

$$D_w := \sum_{e \in E} \epsilon_e D_e. \quad (3.60)$$

Theorem 3.41. *If f and g are Lipschitz functions with Lipschitz constant k_f and k_g , respectively, and $\left(k_g + \|L_w\|k_f\|\Gamma^T\|\right) < 1$, then any trajectory of the CDSH represented by the model of Equation (3.56) achieves synchronization asymptotically. If $f = g$ and $\Gamma = I_k$, then the sufficient condition for synchronization becomes $\|I_N + L_w\| < \frac{1}{k_f}$.*

Proof. Recall that $s_1 = \frac{1}{N} \sum_{i=1}^N u(1)(i)$ and $v(1)$ be an $N \times k$ matrix whose all the N rows be the N copies of s_1 . The trajectory of $\{v(n)\}$ evolves governed by the CDSH model of Equation (3.59), that is, by the equation

$$v(n+1) = g(v(n)) + L_w(f(v(n)))\Gamma. \quad (3.61)$$

As $v(n)$ has equal rows (components) and the same dynamics is going on in each vertex of the systems on hypergraphs, the trajectory $\{v(n)\}$ is confined in the manifold of synchronization, H .

If $\{u(n)\}_{n \in \mathbb{N}}$ be any trajectory of the discrete CDSH governed by Equation (3.59) then by Equation (3.24), Equation (3.61) we have $e(n+1) = (g(u(n)) - g(v(n))) + L_w((f(u(n))) - (f(v(n))))\Gamma$. Therefore, the norm of the error is, $\|e(n+1)\| = \|(g(u(n)) - g(v(n))) + L_w((f(u(n))) - (f(v(n))))\Gamma\| \leq \left(k_g + \|L_w\|k_f\|\Gamma^T\|\right)\|e(n)\|$.

Accordingly, the succession of error $\{e(n)\}_{n \in \mathbb{N}}$ sticks to the following inequality of norms $\|e(n+1)\| \leq \left(k_g + \|L_w\|k_f\|\Gamma^T\|\right)\|e(n)\|$. Moreover, if $f = g$ and $\Gamma = I_k$, then the error inequality becomes $\|e(n+1)\| \leq \left\| \left(I_N + L_w \right) \right\| k_f \|e(n)\|$. Thus, the theorem follows. \square

Corollary 3.42. *If f and g are Lipschitz functions with Lipschitz constant k_f and k_g , respectively, and $\left(k_g + \mu_{\max}k_f\|\Gamma^T\|\right) < 1$, where μ_{\max} is the maximum of the absolute values of the eigenvalues of L_w , then any trajectory of the CDSH represented by the model of Equation (3.56) achieves synchronization asymptotically. If $f = g$ and $\Gamma = I_k$, then the sufficient condition for synchronization becomes $\omega < \frac{1}{k_f}$, where ω is the maximum of the absolute values of the eigenvalues of the matrix $(I_N + L_w)$.*

Proof. The proof directly follows from the Theorem 3.41 and the fact that the operator norm of a symmetric matrix is the maximum of the absolute values of its eigenvalues. \square

By the Remark 3.40.(1), $-L_w$ is positive semi-definite and thus, there exists an orthogonal matrix Δ_w , such that, $\Delta_w^2 = -L_w$. Thus, we have the following.

Lemma 3.43. *There exists a orthogonal matrix Δ_w , which commutes with the matrix L_w . Moreover if the functions \bar{f} and \bar{g} , described in Equation (3.10), are differentiable with all their partial derivatives exist and bounded then $\|\Delta_w f(u(n))\|^2 \leq \|\sup \bar{f}'\|^2 \|\Delta_w u(n)\|^2$ and $\|\Delta_w g(u(n))\|^2 \leq \|\sup \bar{g}'\|^2 \|\Delta_w u(n)\|^2$, where $\|\sup \bar{f}'\|^2 = \left(\sum_{i \in \mathbb{N}_k} \|\sup(\bar{f}'_i)\|^2 \right)$ and $\|\sup \bar{g}'\|^2 = \left(\sum_{i \in \mathbb{N}_k} \|\sup(\bar{g}'_i)\|^2 \right)$.*

Proof. The proof is similar to the same of Lemma 3.14. \square

Now we define $\theta_w(n) := \Delta_w u(n)$, which acts as a lyapunov function in global analysis of the weighted discrete dynamical system.

Lemma 3.44. *If $\theta_w(n) = \Delta_w u(n)$, then $\theta_w(n) \rightarrow 0$ as $n \rightarrow \infty$ implies that the trajectory $\{u(n)\}_{n \in \mathbb{N}}$ achieves synchronization asymptotically.*

Proof. The proof is similar to the same of Lemma 3.15. \square

Theorem 3.45. *If f and g are differentiable functions and $\left[\|\sup \bar{g}'\| + \|\Gamma^T\| \|L_w\| \|\sup \bar{f}'\|\right] < 1$ then any trajectory of the CDSH represented by the model of Equation (3.59) achieves synchronization asymptotically.*

Proof. Using Equation (3.59), we have $\theta_w(n+1) = \Delta_w[g(u(n)) + L_w(f(u(n)))\Gamma]$. Consequently, by using Lemma 3.43 and proceeding as the proof of Theorem 3.16, we get $\|\theta_w(n+1)\| = \|\Delta_w[g(u(n)) + L_w(f(u(n)))\Gamma]\| \leq \left[\|\sup \bar{g}'\| + \|\Gamma^T\| \|L_w\| \|\sup \bar{f}'\|\right] \|\theta_w(n)\|$. Therefore, the theorem follows. \square

Corollary 3.46. *If $f = g$, $\Gamma = cI_k$, and $\|I_N + cL_w\| < \frac{1}{\|\sup \bar{f}'\|}$ then the trajectories of the CDSH, given by Equation (3.59) globally synchronize asymptotically.*

Proof. As $f = g$ and $\Gamma = cI_k$, then using Equation (3.59), we have $\theta_w(n+1) = \Delta_w[I_N + cL_w]f(u(n))$. Therefore, by using Lemma 3.43 we have $\|\theta_w(n+1)\| \leq \|I_N + cL_w\| \|\sup \bar{f}'\| \|\theta_w(n)\|$. Thus, the result follows. \square

Now we state the analogue of Theorem 3.24 for the weighted case.

Theorem 3.47. *Let f is a function of the form given by Equation (3.10) with $\|\bar{f}(x) - \bar{f}(y)\| \leq k_f \|x - y\|$, where \bar{f} is a Lipschitz function. Let $f = g$ and $\Gamma = I_k$. If there exists a negative semidefinite matrix R whose row sum is 0, and there exists a positive real $b > k_f$ such that $(I_N + L_w)^T R (I_N + L_w) - \frac{1}{b^2} R \geq 0$ then the trajectories CDSH, described in Equation (3.59) synchronizes.*

Proof. The proof similar as the same of Theorem 3.24. \square

3.2.2. Stability analysis of the coupled discrete dynamical systems on weighted hypergraphs.

Lemma 3.48. *The stability of synchronization of a synchronized trajectory and the local synchronizability of a trajectory which starts very near to the manifold of synchronization of the CDSH, given in Equation (3.59) depend on the local stability of a dynamical system around 0.*

Proof. Let $u(1) \in \mathbb{R}^{Nk}$ be a point very close to the manifold of synchronization, H . There exists a point $v(1) \in H \subset \mathbb{R}^{Nk}$ such that $e(1) = u(1) - v(1)$ and $\|e(1)\|$ is sufficiently small. Let $\{u(n)\}_{n \in \mathbb{N}}$ and $\{v(n)\}_{n \in \mathbb{N}}$ be two trajectories of the CDSH represented by Equation (3.59) with the initial points $u(1)$ and $v(1)$, respectively, and $\{e(n)\}_{n \in \mathbb{N}}$ be the trajectory of another dynamical system defined by $e(n) = u(n) - v(n)$. Using Equation (3.59) we have,

$$\begin{aligned} e(n+1) &= [g(u(n)) + L_w f(u(n))\Gamma] - [g(v(n)) + L_w f(v(n))\Gamma] \\ &= g(u(n)) - g(v(n)) + L_w [f(u(n)) - f(v(n))]\Gamma. \end{aligned} \quad (3.62)$$

As $v(1) \in H$, by Equation (3.59), we get $v(n) \in H$ for all $n \in \mathbb{N}$. Now if $e(n) \rightarrow 0$, as $n \rightarrow \infty$, then the local synchronization is achieved by the trajectory $\{u(n)\}_{n \in \mathbb{N}}$ and the synchronization of the synchronized trajectory $\{v(n)\}_{n \in \mathbb{N}}$ is stable under a small perturbation.

Therefore, Equation (3.41) and Equation (3.39) together imply,

$$e(n+1) = e(n)J_g(n) + L_w e(n)J_f(n)\Gamma. \quad (3.63)$$

Thus, Equation (3.63) represents the required dynamical system, whose stability around 0 is equivalent to local stability of synchronization of the synchronized solution of the weighted CDSH, given by Equation (3.59). \square

As L_w is a symmetric matrix, there exists an orthogonal matrix R (The rows of R are the eigenvectors of L_w) such that $L_w = R^T D_{L_w} R$, where D_{L_w} is the diagonalization of L_w . Multiplying R on the both sides of Equation (3.63) we get, $Re(n+1) = Re(n)J_g(n) + RL_w R^T Re(n)J_f(n)\Gamma$. Thus,

$$\eta_w(n+1) = \eta_w(n)J_g(n) + D_{L_w} \eta_w(n)J_f(n)\Gamma, \quad (3.64)$$

where $\eta_w(n) = Re(n)$ for all $n \in \mathbb{N}$. Clearly which implies $\eta_w(n+1)(i) = \eta_w(n)(i)J_g(n) + \mu_i \eta_w(n)(i)J_f(n)\Gamma$. Therefore,

$$\eta_w(n+1)(i) = \left\{ \prod_{k=1}^n (J_g(k) + \mu_i J_f(k)\Gamma) \right\} \eta_w(1)(i) \quad (3.65)$$

for all $i \in \mathbb{N}_N$, where $\{\mu_i\}_{i \in \mathbb{N}_N}$ are all the eigenvalues of L_w . Clearly $e(n) \rightarrow 0$ as $n \rightarrow \infty$ if $\eta_w(n) \rightarrow 0$ as $n \rightarrow \infty$. Thus, the condition of local synchronization of $\{u(n)\}_{n \in \mathbb{N}}$ and the condition of stability of the synchronization of $\{v(n)\}_{n \in \mathbb{N}}$ are the condition of stability of $\{\eta_w(n)_i\}_i$ for all $i \in \mathbb{N}_N$ around the equilibrium point 0.

Theorem 3.49. *The synchronization of the synced trajectory $\{v(n)\}_{n \in \mathbb{N}}$ of CDSH given by Equation (3.59) is stable under a small perturbation if and only if $\|(J_g(n) + \mu_i J_f(n)\Gamma)\|_A < 1$.*

Proof. The result follows by replacing $\epsilon \lambda_i$ by μ_i in the proof of Lemma 3.26. \square

Corollary 3.50. *Let the limit, $\sigma = \lim_{n \rightarrow \infty} \frac{1}{n} \sum_{r=1}^n \log \|J_f(r)\|_A$ exists and $f = g$ and $\Gamma = cI_k$, for some constant c . The synchronization of the synced trajectory $\{v(n)\}_{n \in \mathbb{N}}$ of CDSH described in Equation (3.59) is stable under a small perturbation if all the absolute values of the eigenvalues of L_w are contained in the interval $[\frac{1-e^{-\sigma}}{c}, \frac{1+e^{-\sigma}}{c}]$.*

Proof. If $g = f$ and $\Gamma = I_k$, then by Equation (3.65) we have,

$$\eta_w(n+1)(i) = \left[\prod_{k=1}^n (1 + c\mu_i) J_f(k) \right] \eta_w(1)(i). \quad (3.66)$$

Let $\sigma = \lim_{n \rightarrow \infty} \frac{1}{n} \left[\sum_{k=1}^n \log \|J_f(k)\| \right]$. Now Equation (3.66) implies that

$$\|\eta_w(n+1)(i)\| = \left[(1 + \mu_i c) e^\sigma \right]^n \|\eta_w(1)(i)\|. \quad (3.67)$$

Thus, the trajectories synchronize locally if $|(1 + \mu_i)e^\sigma| < 1$ for all i , that is equivalent to $(1 - e^{-\sigma}) < -c\mu_i < (1 + e^{-\sigma})$. Thus, the result follows. \square

Remark 3.51. Recall Remark 3.28, where we have described a correspondence between the rows of $Qe(1)$ and the eigenvalues of C . Similarly there is a correspondence between the rows of $Re(1)$ and the eigenvalues of L_w . We are going to use this correspondence in the next result.

Now we will state a result, which is analogous to Theorem 3.29.

Theorem 3.52. Let the limit, $\sigma = \lim_{n \rightarrow \infty} \frac{1}{n} \sum_{r=1}^n \log \|J_f(r)\|_A$ exists and $f = g$, $\Gamma = c.I_k$, for some constant $c > 0$. Let $e(1)$ be the initial perturbation of synchronized trajectory. The synchronization of the synced trajectory $\{v(n)\}_{n \in \mathbb{N}}$ of CDSH given by Equation (3.59) is stable under a small perturbation if and only if either the i -th row (component) of the $Re(1) = \eta_w(1)$ is zero or the absolute value of the corresponding i -th eigenvalue of L_w is contained in the interval $[\frac{1-e^{-\sigma}}{c}, \frac{1+e^{-\sigma}}{c}]$.

Proof. Similar to the proof of Theorem 3.29. \square

Corollary 3.53. Let the limit, $\sigma = \lim_{n \rightarrow \infty} \frac{1}{n} \sum_{r=1}^n \log \|J_f(r)\|_A$ exists and $f = g$, $\Gamma = c.I_k$, for some constant $c > 0$. The synchronization of the synced trajectory $\{v(n)\}_{n \in \mathbb{N}}$ of CDSH given by Equation (3.59) is stable under a small perturbation if all the absolute values of the nonzero eigenvalues of L_w are contained in the interval $[\frac{1-e^{-\sigma}}{c}, \frac{1+e^{-\sigma}}{c}]$.

Proof. Similar to the proof of Corollary 3.31. \square

Theorem 3.54. If there exists a positive definite matrix A such that $[((J_g(n) + \mu_i J_f(n)\Gamma))A((J_g(n) + \mu_i J_f(n)\Gamma))^T - A] < 0$ for all i then local synchronization is achieved by any trajectory $\{u(n)\}_{n \in \mathbb{N}}$ and the synchronization of the synchronized trajectory $\{v(n)\}_{n \in \mathbb{N}}$ of CDSH, given by Equation (3.59), is stable under small perturbation.

Proof. The proof follows by replacing $\epsilon\lambda_i$ by μ_i in the proof of Theorem 3.36. \square

Thus, by using Lemma 3.33 and Lemma 3.35 we have the following corollary.

Corollary 3.55. If there exists a positive definite matrix A such that

$$\begin{pmatrix} A & (J_g(n) + \mu_i J_f(n)\Gamma) \\ (J_g(n) + \mu_i J_f(n)\Gamma)^T & A^{-1} \end{pmatrix} > 0$$

for all i then local synchronization is achieved by any trajectory $\{u(n)\}_{n \in \mathbb{N}}$ and the synchronization of the synchronized trajectory $\{v(n)\}_{n \in \mathbb{N}}$ of CDSH, given by Equation (3.16), is stable under a small perturbation.

3.3. Structural property of the hypergraph and synchronizability. In this subsection we conclude some results on the influence of the structure of the underlying (unweighted) hypergraph topology on local synchronization. We start with two results from [4].

Theorem 3.56. [4, Theorem 3.5] For a connected hypergraph G with N vertices,

$$\text{diam}(G) \geq \frac{4}{N(m_{\max} - 1)\lambda_{\min}}$$

where λ_{\min} is the minimum non-zero eigen value of L_G .

Theorem 3.57. [4, Theorem 3.8] For a connected m -uniform hypergraph with N vertices $\lambda_{\max} \leq \max \left\{ \frac{2d(i)(m-1)-1+\sqrt{4(m-1)^2d(i)m_i D_{\max}^2 - 2d_i(m-1)+1}}{2(m-1)} : v_i \in V \right\}$, where $m_i = \frac{(\sum_{j \sim i} d(j))}{d(i)(m-1)}$ and $D_{\max} = \max\{d_{ij} = \text{number of edge containing both } v_i, v_j : v_i, v_j \in V\}$.

From now, we denote the quantity $\max \left\{ \frac{2d(i)(m-1)-1+\sqrt{4(m-1)^2d(i)m_i D_{\max}^2 - 2d_i(m-1)+1}}{2(m-1)} : v_i \in V \right\}$ by b_m . The following result directly follows from Corollary 3.32 and Theorem 3.56.

Proposition 3.58. If $f = g$, $\Gamma = c.I_k$ for some constant $c > 0$, the limit $\sigma = \lim_{n \rightarrow \infty} \frac{1}{n} \sum_{r=1}^n \log \|J_f(r)\|_A$ exists, and the coupling strength ϵ is contained in the interval $[N(m_{\max} - 1)\text{diam}(G)\frac{1-e^{-\sigma}}{4c}, \frac{1+e^{-\sigma}}{c\lambda_{\max}}]$, where λ_{\max} is the maximum of the absolute values of the nonzero eigenvalues of C respectively then local synchronization is achieved by any trajectory $\{u(n)\}_{n \in \mathbb{N}}$ and the synchronization of the synchronized trajectory $\{v(n)\}_{n \in \mathbb{N}}$ of the CDSH, given by Equation (3.16) is stable under small perturbation.

Corollary 3.32, Theorem 3.56 and Theorem 3.57 lead us to the following result.

Theorem 3.59. *If the underlying hypergraph is a connected m -uniform hypergraph and $f = g$, $\Gamma = cI_k$ for some constant $c > 0$, the limit $\sigma = \lim_{n \rightarrow \infty} \frac{1}{n} \sum_{r=1}^n \log \|J_f(r)\|_A$ exists, and the coupling strength ϵ is contained in the interval $[N(m-1)\text{diam}(G)\frac{1-e^{-\sigma}}{4c}, \frac{1+e^{-\sigma}}{cb_m}]$, then local synchronization is achieved by any trajectory $\{u(n)\}_{n \in \mathbb{N}}$ and the synchronization of the synchronized trajectory $\{v(n)\}_{n \in \mathbb{N}}$ of the CDSH, given by Equation (3.16) is stable under small perturbation.*

3.4. Coupled continuous dynamical systems on hypergraphs. While developing the models for coupled discrete dynamical systems on hypergraph, we have used some diffusion matrices of hypergraphs, such as C and L_w . Now using these matrices and following the existing methods for constructing models for continuous-time dynamical networks, we build the same for continuous-time CDSH. We start with weighted case using the matrix $L_w = \sum_{e_r \in E} \epsilon_{e_r} H_{e_r}$. The same for an unweighted systems on hypergraphs will automatically follow by taking the coupling strengths as constant, i.e., $\epsilon_{e_r} = \epsilon$ for all $e_r \in E$. Then $L_w = \epsilon C$.

The model of the continuous-time CDSH is given by the equation

$$\dot{u}(t) = f(u(t)) + L_w g(u(t)) \Gamma, \quad (3.68)$$

where f, g, u are as described in Equation (3.9) and Equation (3.10), and Γ is described in Equation (3.16). We use t to denote the time instead of n , to distinguish between the discrete and continuous-time cases. Now we start with local stability analysis.

3.4.1. Local stability analysis of coupled continuous-time dynamical systems on hypergraphs. Let $s_1 = \frac{1}{N} \sum_{i=1}^N u(1)(i) (\in \mathbb{R}^k)$ and $v(1)$ be an $N \times k$ matrix whose all the N rows are N copies of s_1 . Let $\{v(n)\}$ be a trajectory that evolves by the rules of the CDSH model described in Equation (3.68). Clearly, the trajectory $\{v(n)\}$ starts from the manifold of synchronization and confined in this manifold. Thus, if any trajectory becomes closer to $\{v(n)\}$ with the flow of time then that trajectory synchronizes asymptotically. Now taking $e(t) = u(t) - v(t)$ we have

$$\dot{e}(t) = f(u(t)) - f(v(t)) + L_w(g(u(t)) - g(v(t))) \Gamma. \quad (3.69)$$

We recall Equation (3.42). As the trajectories $u(t)$ and $v(t)$ are very close, we use linearized approximation and, thus, we write

$$g(u(t)) = g(v(t)) + e(t) \cdot J_g(t) \quad \text{and} \quad f(u(t)) = f(v(t)) + e(t) \cdot J_f(t). \quad (3.70)$$

Therefore, Equation (3.69) becomes

$$\dot{e}(t) = e(t) \cdot J_f(t) + L_w(e(t) \cdot J_g(t)) \Gamma. \quad (3.71)$$

L_w is a symmetric matrix. Thus, there exists an orthogonal matrix R such that $L_w = R^T D_{L_w} R$, where D_{L_w} is the diagonalization of L_w . Multiplying R on the both sides of Equation (3.71) we get, $R\dot{e}(t) = Re(t) \cdot J_f(t) + RL_w R^T Re(t) \cdot J_g(t) \Gamma$, which implies $\dot{\eta}_w(t) = \eta_w(t) \cdot J_f(t) + D_{L_w} \eta_w(t) \cdot J_g(t) \Gamma = \eta_w(t)(i) \cdot J_f(t) + \mu_i \eta_w(t)(i) \cdot J_g(t) \Gamma$. Therefore,

$$\dot{\eta}_w(t)(i) = \eta_w(t)(i) \cdot [J_f(t) + \mu_i J_g(t) \Gamma] \quad (3.72)$$

for all $i \in \mathbb{N}_N$. Now from the above discussion we have the following theorem.

Theorem 3.60. *If the system described in Equation (3.72) is asymptotically stable around its zero solution, then the synchronization of a synchronized trajectory of the CDSH described in Equation (3.68) is stable under small perturbation.*

Now using the Lyapunov approach, we have some sufficient conditions for ensuring the stability of the synchronization.

Theorem 3.61. *If there exists a positive definite $k \times k$ matrix P and a positive real b such that for all i, t , $[J_f(t) + \mu_i J_g(t) \Gamma + bI_k]P$ is a negative semidefinite matrix then synchronization in the CDSH given by Equation (3.68) is stable under small perturbation.*

Proof. Let us consider the Lyapunov function $W_{P_i}(t) = \frac{1}{2} \eta_w(t)(i) P \eta_w(t)^T(i)$, where P is a $k \times k$ positive definite matrix. Then

$$\begin{aligned} \dot{W}_{P_i}(t) &= \dot{\eta}_w(t)(i) P \eta_w^T(t)(i) = \eta_w(t)(i) [J_f(t) + \mu_i J_g(t) \Gamma] P \eta_w^T(t)(i) \\ &\leq -b \eta_w(t)(i) P \eta_w(t)^T(i) = -2b W_{P_i}(t). \end{aligned} \quad (3.73)$$

Therefore, $W_{P_i}(t) \rightarrow 0$ as $t \rightarrow \infty$ for all i , and this completes the proof. \square

Note that for $k = 1$, the condition in Theorem 3.61 becomes as follows If there exists a $b > 0$ such that $[\frac{d\bar{f}(s_t)}{dt} + \mu_i \frac{d\bar{g}(s_t)}{dt} + b] \leq 0$. Thus, we state the following.

Corollary 3.62. *If $k = 1$, $\Gamma = 1$, and there exists a positive real b such that for all i, t , $[\frac{d\bar{f}(s_t)}{dt} + \mu_i \frac{d\bar{g}(s_t)}{dt} + b] \leq 0$ then synchronization in the CDSH, given by Equation (3.68) is stable under small perturbation.*

Using the vector notation for $u(t)$ and $v(t)$ instead of the matrix notation, we can conclude the following result.

Theorem 3.63. *The synchronization of a synchronized trajectory of the CDSH given by Equation (3.68) is stable under small perturbation if $[J_f(t) \otimes I_N + J_g(t) \otimes D_{L_w}]$ is negative definite, where \otimes is Kronecker product and D_{L_w} is the diagonalization of L_w .*

Proof. Let us consider a Lyapunov function $V_I(t) = \frac{1}{2} \sum_{i \in \mathbb{N}_N} (\eta_w(t)(i))(\eta_w(t)(i))^T$. Differentiating $V_I(t)$ with respect to t we get

$$\begin{aligned} \dot{V}_I(t) &= \sum_{i \in \mathbb{N}_N} (\dot{\eta}_w(t)(i))(\eta_w(t)(i))^T = \sum_{i \in \mathbb{N}_N} \eta_w(t)(i) \cdot [J_f(t) + \mu_i J_g(t)\Gamma](\eta_w(t)(i))^T \\ &= \eta_w(t)[J_f(t) \otimes I_N + J_g(t) \otimes D_{L_w}]\eta_w(t)^T. \end{aligned} \quad (3.74)$$

As $[J_f(t) \otimes I_N + J_g(t) \otimes D_{L_w}]$ is negative definite, $\dot{V}_I(t) < 0$ and therefore, the result follows. \square

3.4.2. *Global synchronization in continuous-time CDSH.* Here, we restrict g as an identity function. Thus, Equation (3.69) becomes

$$\dot{e}(t) = f(u(t)) - f(v(t)) + L_w(e(t))\Gamma. \quad (3.75)$$

Thus, the evolution of the i -th vertex is expressed by

$$\dot{e}(t)(i) = \bar{f}(u(t)(i)) - \bar{f}(v(t)(i)) + \sum_{j \in \mathbb{N}_N} L_{wij}(e(t)(j))\Gamma. \quad (3.76)$$

Theorem 3.64. *If Γ is positive semidefinite diagonal matrix and there exists a $k \times k$ diagonal positive definite matrix P such that $(\bar{f}(x) - \bar{f}(y))P(x - y)^T \leq (x - y)k(P, \bar{f})(x - y)^T$ where $K(P, \bar{f})$ is negative definite, then any trajectory of the dynamical system given by Equation (3.68) synchronizes asymptotically.*

Proof. Let us consider a Lyapunov function $V_P(t) = \frac{1}{2} \sum_{i \in \mathbb{N}_N} (e(t)(i))P(e(t)(i))^T$. Now differentiating $V_P(t)$ with respect to t and by using Equation (3.76), we have

$$\begin{aligned} \dot{V}_P(t) &= \sum_{i \in \mathbb{N}_N} [\bar{f}(u(t)(i)) - \bar{f}(v(t)(i)) + \sum_{j \in \mathbb{N}_N} L_{wij}(e(t)(j))\Gamma]P(e(t)(i))^T \\ &\leq \sum_{i \in \mathbb{N}_N} (e(t)(i))k(P, \bar{f})(e(t)(i))^T + \sum_{i \in \mathbb{N}_N} \sum_{j \in \mathbb{N}_N} L_{wij}(e(t)(j))\Gamma P(e(t)(i))^T \\ &= \sum_{i \in \mathbb{N}_N} (e(t)(i))k(P, \bar{f})(e(t)(i))^T + \sum_{i \in \mathbb{N}_N} \sum_{j \in \mathbb{N}_N} L_{wij} \sum_{r \in \mathbb{N}_k} (e(t)(j))(r)\Gamma_{rr}P_{rr}(e(t)(i)(r)) \end{aligned} \quad (3.77)$$

$$= \sum_{i \in \mathbb{N}_N} (e(t)(i))k(P, \bar{f})(e(t)(i))^T + \sum_{r \in \mathbb{N}_k} \Gamma_{rr}P_{rr}(e(t)(\cdot, r))^T L_w(e(t)(\cdot, r)). \quad (3.78)$$

$\dot{V}_P(t) < 0$, as L_w is negative semidefinite, Γ is positive semidefinite, P is positive definite, and $k(P, \bar{f})$ is negative definite. Thus, $V_P(t) \rightarrow 0$ as $t \rightarrow \infty$. Therefore, the result follows. \square

Example 3.65. *Let \bar{f} be a differentiable function which has bounded partial derivatives. Let $\sup(f') = \{\sup_t \frac{\partial \bar{f}^i(s_i)}{\partial x^j}\}_{i,j \in \mathbb{N}_k}$ and there exists a positive definite matrix P such that $\sup(f')P$ is negative semidefinite. Now if we take $k(P, \bar{f}) = \sup(f')P$ then the condition given in Theorem 3.64 is satisfied.*

Theorem 3.66. *If $\Gamma = I_k$ and $(\bar{f}(x) - \bar{f}(y))(x - y)^T \leq (x - y)k(I, \bar{f})(x - y)^T$ where $K(I, \bar{f}) + L_w$ is negative definite, then the trajectories of the dynamical system given by Equation (3.68) synchronize asymptotically.*

Proof. Take $P = \Gamma = I_k$ in Equation (3.77) we get

$$\dot{V}_I(t) \leq \sum_{i \in \mathbb{N}_N} (e(t)(i))k(I, \bar{f})(e(t)(i))^T + \sum_{i \in \mathbb{N}_N} \sum_{j \in \mathbb{N}_N} L_{wij}(e(t)(j))(e(t)(i))^T. \quad (3.79)$$

If we consider $e(t)$ in vector form then from Equation (3.77) we have $\dot{V}_I(t) \leq e(t)k(I, \bar{f}) \otimes I_k e(t)^T + e(t)L_w \otimes I_k (e(t))^T = e(t)[k(I, \bar{f}) \otimes I_k + L_w \otimes I_k]e(t)^T = e(t)[(k(I, \bar{f}) + L_w) \otimes I_k]e(t)^T$. As $(k(I, \bar{f}) + L_w)$ is negative definite, $\dot{V}_I(t)$ is negative and $V_I(t) \rightarrow 0$, as $t \rightarrow \infty$. thus, the result follows. \square

Remark 3.67. *The results derived from Theorem 3.64 and Theorem 3.66 by taking $m_{\max} = 2$ (that is when the underlying hypergraph becomes graph) are similar to what have been reported in [17, 30].*

In the next result, we consider $k = 1$. Thus, Γ is a scalar. For simplicity we assume $\Gamma = 1$. Now Equation (3.68) becomes

$$\dot{u}(t) = f(u(t)) + L_w g(u(t)). \quad (3.80)$$

Thus, Equation (3.69) becomes

$$\dot{e}(t) = f(u(t)) - f(v(t)) + L_w(g(u(t)) - g(v(t))). \quad (3.81)$$

Theorem 3.68. *For $k = 1$, If there exists an $N \times N$ positive definite matrix P such that $(x-y)^T P(f(x) - f(y)) \leq (x-y)^T k_{(P,f)}(x-y)$ and $(x-y)^T P L_w(g(x) - g(y)) \leq (x-y)^T k_{(P,L_w,g)}(x-y)$, for all $x, y \in \mathbb{R}^N$, where both $k_{(P,L_w,g)}$, and $k_{(P,f)}$ are $N \times N$ matrix and $[k_{(P,f)} + k_{(P,L_w,g)} + bP]$ is a negative definite matrix, then any trajectory of the CDSH given by Equation (3.80) synchronizes.*

Proof. Let us consider the quantity $V_w(t) = \frac{1}{2}(e(t))^T P e(t)$, where P is an $N \times N$ positive definite matrix. So $\lim_{t \rightarrow 0} V_w(t) = 0 \implies \lim_{t \rightarrow 0} e(t) = 0$. Now $\dot{V}_w(t) = (e(t))^T P \dot{e}(t) = (e(t))^T P [f(u(t)) - f(v(t)) + L_w(g(u(t)) - g(v(t)))] \leq (e(t))^T [k_{(P,f)} + k_{(P,L_w,g)}] e(t) \leq -b(e(t))^T P e(t) = -2bV_w(t)$. Therefore, $\lim_{t \rightarrow 0} V_w(t) = 0$ and this completes the proof. \square

3.5. CDSH models using normalized matrices. The use of normalized Laplacian matrices in a dynamical network model is quite common. We can also construct the same for systems on hypergraphs by using a normalized matrices associated with its underlying hypergraph, for both, discrete-time and continuous-time dynamical systems. It is also common to multiply the Laplacian matrix by the inverse of the degree matrix to obtain the normalized Laplacian matrix (see Definition 2.5). As the hypergraph G is connected, the matrices, D_G , and D_w are positive definite and thus, are invertible. Here D_G is the degree matrix of G and D_w is defined in Equation (3.60).

Similar to Definition 2.5, we define

$$\hat{C} := D_G^{-1} C \text{ and } \hat{L} := D_w^{-1} L_w. \quad (3.82)$$

As, the row sums of both the matrices, \hat{C} and \hat{L} are zero, so the diffusion process in a systems on hypergraphs and the related synchronization can be described using these matrices. Now if we replace C and L_w by \hat{C} and \hat{L} , respectively, all the models described in the previous sections, become CDSH models involving the normalized matrices.

Remark 3.69. *In previous sections, we have used the fact that C and L_w are symmetric, but, in general, \hat{C} and \hat{L} are not. Though, both of them are not symmetric with respect to the usual inner product, but, \hat{C} and \hat{L} are symmetric with respect to the inner products $\langle \cdot, \cdot \rangle_{D_G}$ and $\langle \cdot, \cdot \rangle_{D_w}$, respectively, where $\langle x, y \rangle_{D_G} := x^T D_G y$ and $\langle x, y \rangle_{D_w} = x^T D_w y$ for all $x, y \in \mathbb{R}^N$. Thus, using these inner products we can derive the similar results by using \hat{C} and \hat{L} in places of C and L_w , respectively, in previous sections.*

4. COMPARISON WITH GRAPH-MODELS

We intend to incorporate multi-body interactions using the underlying topology of the dynamical network in our work. Generally, a graph (or a network) is used as the underlying topology of dynamical networks. We use hypergraph as the underlying topology. A hypergraph is a generalization of a graph and if we take the maximum edge cardinality of a hypergraph, $m_{\max} = 2$, it becomes a graph. Thus our model is so adaptable that we can get back to the graph case when it is needed. It is important to note that in many situations, the interactions in a network are multi-nary. Using binary interactions, we approximate those multi-nary synergies. For example, in the synchronized chirping of crickets, in the synchronous flashing of a swarm of male fireflies, the interactions are multi-nary. Diffusion of any substance (for example ink) on a surface (for example on a piece of cloth) can be described conveniently using grids on that surface. The grids are indeed hypergraphs. The hypergraph representation of a grid is described in Example 5.3. suppose that we put a drop of ink on one of the cells in the grid. As the ink spreads in all the neighboring cells, the interaction is multi-nary and can be described conveniently by a hyperedge containing the cell and its neighbors. Though sometimes multi-nary interaction can be approximated by multiple binary interactions, the approximation may not work in some situations. To illustrate this we consider an abstract example where a 3-uniform hyperedge, e (Figure 1a) is approximated by three 2-edges (drawn with the dotted lines in Figure 1a). The corresponding diffusion matrix L (which is the negative of Laplacian) of the triangle is $\begin{pmatrix} -2 & 1 & 1 \\ 1 & -2 & 1 \\ 1 & 1 & -2 \end{pmatrix}$. The matrix $C = H_e$ corresponding to the edge e is $\begin{pmatrix} -1 & \frac{1}{2} & \frac{1}{2} \\ \frac{1}{2} & -1 & \frac{1}{2} \\ \frac{1}{2} & \frac{1}{2} & -1 \end{pmatrix}$. Now the discrete diffusion equation expressed by L is

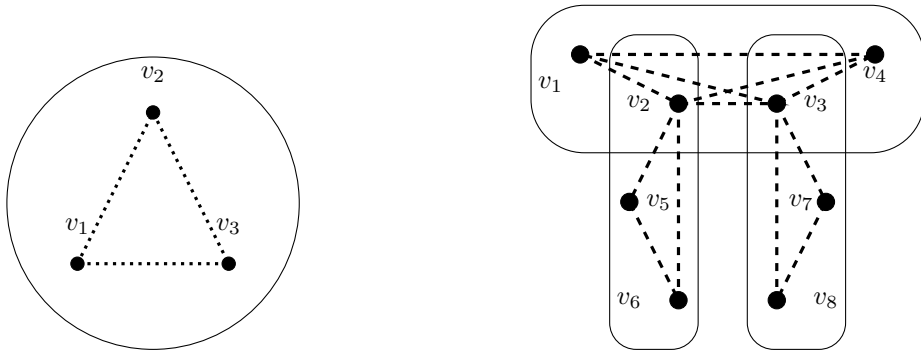
$$x(n+1) = x(n) + L(x(n)), \quad (4.1)$$

and the same described by C is

$$x(n+1) = x(n) + C(x(n)). \quad (4.2)$$

The eigenvalues of $I_3 + L$ are $-2, -2, 1$ and the same of $I_3 + C$ are $-\frac{1}{2}, -\frac{1}{2}, 1$. The trajectories of the system given by Equation (4.2) synchronize because for the matrix $I_3 + C$ the eigenspace of 1 is the vector space

generated by the vector $\mathbf{1}$ and the magnitude of the other eigenvalues is less than 1. The same is not valid for Equation (4.1) because the magnitudes of the eigenvalues (other than 1) of $I_3 + L$ are greater than 1.



(A) A 3-hyperedge is approximated by a triangle (B) Approximation of a hypergraph topology by a graph

FIGURE 1. Comparison between a hypergraph and its underlying graph

The matrix C corresponding to the hypergraph in Figure 1a coincides with the negative normalized Laplacian matrix (defined in [22, Equation-2]) of the triangle graph. In general, the matrix C is different from this notion of normalized Laplacian because C is symmetric for any hypergraph whereas the normalized Laplacian is not symmetric for non-regular graphs. Next, we consider another abstract example where binary interactions fails to approximate multi-nary interactions. We approximate the hypergraph by a graph whose edges are drawn with the dashed lines (see Figure 1b). The diffusion matrix C of the hypergraph and the negative

Laplacian matrix L of the underlying graph approximation are as follows.
$$C = \begin{pmatrix} -1 & \frac{1}{3} & \frac{1}{3} & \frac{1}{3} & 0 & 0 & 0 & 0 \\ \frac{1}{3} & -2 & \frac{1}{3} & \frac{1}{3} & \frac{1}{2} & \frac{1}{2} & 0 & 0 \\ \frac{1}{3} & \frac{1}{3} & -2 & \frac{1}{3} & 0 & 0 & \frac{1}{2} & \frac{1}{2} \\ \frac{1}{3} & \frac{1}{3} & \frac{1}{3} & -1 & 0 & 0 & 0 & 0 \\ 0 & \frac{1}{2} & 0 & 0 & -1 & \frac{1}{2} & 0 & 0 \\ 0 & \frac{1}{2} & 0 & 0 & \frac{1}{2} & -1 & 0 & 0 \\ 0 & 0 & \frac{1}{2} & 0 & 0 & 0 & -1 & \frac{1}{2} \\ 0 & 0 & \frac{1}{2} & 0 & 0 & 0 & \frac{1}{2} & -1 \end{pmatrix},$$

$$L = \begin{pmatrix} -3 & 1 & 1 & 1 & 0 & 0 & 0 & 0 \\ 1 & -5 & 1 & 1 & 1 & 0 & 0 & 0 \\ 1 & -5 & 1 & 1 & 0 & 0 & 1 & 1 \\ 1 & 1 & 1 & -3 & 0 & 0 & 0 & 0 \\ 0 & 1 & 0 & 0 & -2 & 1 & 0 & 0 \\ 0 & 1 & 0 & 0 & 1 & -2 & 0 & 0 \\ 0 & 0 & 1 & 0 & 0 & 0 & -2 & 1 \\ 0 & 0 & 1 & 0 & 0 & 0 & 1 & -2 \end{pmatrix}.$$

Now, we compare the diffusion equations stated using C and L , respectively.

$$x(n+1) = x(n) + \frac{3}{4}C(x(n)). \quad (4.3)$$

$$x(n+1) = x(n) + \frac{3}{4}L(x(n)). \quad (4.4)$$

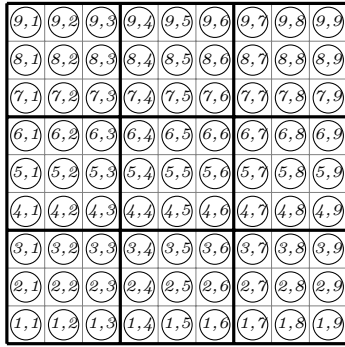
The eigenvalues of the matrix, $I_8 + \frac{3}{4}C$ are $-0.930, -0.678, -0.125, -0.125, 0.867 \times 10^{-17}, 0.553, 0.806, 1$. $\mathbf{1}$ is the eigenvector corresponding to the eigenvalue 1 and the absolute values of the other eigenvalues are less than 1. Therefore, the trajectories of the system given by Equation (4.3) synchronize asymptotically. The eigenvalues of the matrix, $I_8 + \frac{3}{4}L$ are $-3.17, -3.79, -2, -1.25, -1.25, -0.08, 0.53, 1$. So the absolute values of some eigenvalues are greater than 1. Therefore, the trajectories of the system given by Equation (4.4) may not synchronize.

5. NUMERICAL ILLUSTRATIONS

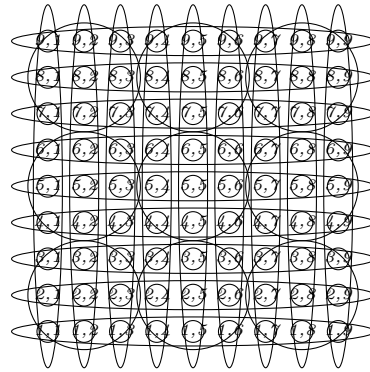
In this section we numerically demonstrate the theoretical results obtained in the previous sections.

5.1. Numerical Simulations. In this subsection, we illustrate our results on synthetic models build on high-order structures. We construct hypergraphs from some virtual situations involve multi-body interactions and explore our theoretical results in the context of those hypergraphs.

5.1.1. Few synthetic hypergraphs. First, we construct some hypergraphs which are used as the underlying architecture of the CDSH, described in the examples of the later subsections.



(A) Sudoku-grid.



(B) Hypergraph representation of sudoku grid.

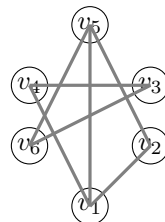
FIGURE 2. Sudoku hypergraph.

Example 5.1. In sudoku grid (Figure 2a) there are 3×3 squares (say, blocks). Each block consists of 3 rows and columns, respectively. So, altogether, a sudoku grid has 81 cells create 9 rows and 9 columns of the grid. We construct a 9-uniform hypergraph G from a sudoku grid, where the 81 cells are considered as the vertices with the following indexing map. The (i, j) -th cell of the grid is taken as the vertex $v_{i+9 \times (j-1)}$ of G . The hyper-edges are (Figure 2b) all the 9 rows, 9 columns, and 9 blocks having 3×3 cells each. We denote a block as $B_{p,q}$, where $p, q = 1, \dots, 3$. Thus, the (i, j) -th cell belongs to the block $B_{p,q}$, where $p = \lceil i/3 \rceil$ and $q = \lceil j/3 \rceil$. So, two vertices (cells), v_i and v_j are adjacent if, either they belong to the same column / row or in the same square block. We index the hyper-edges as follows. For $i = 1, \dots, 9$, the i -th row represents the i -th hyper-edge, i.e. e_i . For $j = 1, \dots, 9$, the $(9+j)$ -th hyper-edge, e_{9+j} , is represented by the j -th column of the grid. For $p, q = 1, \dots, 3$ the $(18 + p + 3 \times (q - 1))$ -th hyper-edge, $e_{18+p+3 \times (q-1)}$, is represented by $B_{p,q}$. Thus, there are 81 vertices and 27 hyper-edges in G . Clearly the incidence matrix I_G is an 81×27 matrix in which the row corresponding to the vertex $v_{i+9 \times (j-1)}$ (cell (i, j)), that is, the $i + 9 \times (j - 1)$ -th row of I_G has 1 in the i -th, $(9 + j)$ -th, and the $(18 + \lceil i/3 \rceil + 3 \times (\lceil j/3 \rceil - 1))$ -th columns, respectively, and has 0 in rest of the columns.

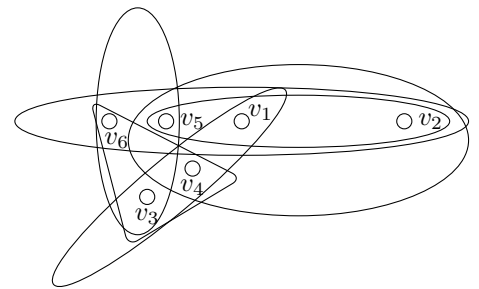
Clearly for this example, the matrix B_9 (defined in Equation (3.8)) is an 81×81 matrix whose eigenvalues are $-\frac{27}{8}$, $-\frac{9}{4}$, $-\frac{9}{8}$, and 0 with multiplicity 60, 16, 4, and 1, respectively.

Example 5.2. Consider the graph in Figure 3a. There are 6 vertices. Now we construct a hypergraph (Figure 3b), with same 6 vertices. A hyper-edge of this hypergraph consists of a vertex of the graph (hypergraph) along with its neighbors in the graph. So, two vertices of the graph are adjacent in the hypergraph if either they are adjacent in the graph or they has a common neighbour in the graph.

Thus, the number of edges in the hypergraph is equal to the number vertices in the graph, (i.e., 6 in Figure 3a). Two of the hyper-edges have cardinality 4 and the rest have the cardinality 3. The connectedness of this hypergraph follows from the connectedness of the graph. We denote the hyper-edge corresponding to the neighbours of the vertex v_i by e_i .



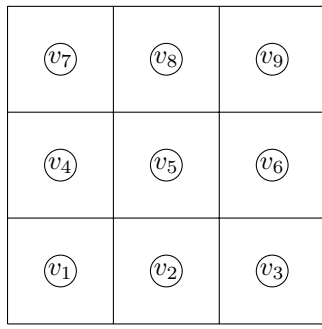
(A) Graph.



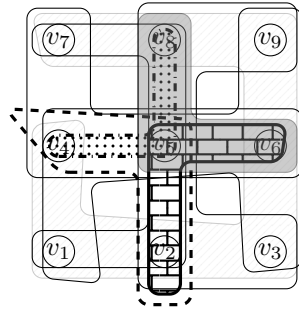
(B) hypergraph.

FIGURE 3. Hypergraph obtained from the neighbourhoods of a graph.

Example 5.3. Let there be a 3×3 grid, i.e., with 9 cells (as shown in Figure 4a). Now we construct a hypergraph. Consider all the cells as vertices. A hyper-edge e_i corresponding to a cell (vertex) v_i consists of only all of its neighbouring cells, i.e. the cells which share a common side or a corner point with the cell v_i (see Figure 4b). Note that, here $v_i \notin e_i$. We denote the hyper-edge corresponding to the vertex v_i as e_i .



(A) 9-grid.



(B) Hypergraph obtained from 9-grid neighbourhoods.

Two vertices are adjacent in the hypergraph if the corresponding cells have a common neighbour. The hyperedge e_5 , has cardinality 8. The four hyperedges $e_4, e_6, e_2,$ and e_8 have the cardinality 5 and the rest of the four hyperedges (i.e., $e_1, e_3, e_9,$ and e_7) are of cardinality 3. The hyperedge e_5 contains all the 8 vertices except v_5 . Thus, considering e_5 along with any other edge containing v_5 shows that the hypergraph is connected.

FIGURE 4. 9-grid neighbourhood hypergraph.

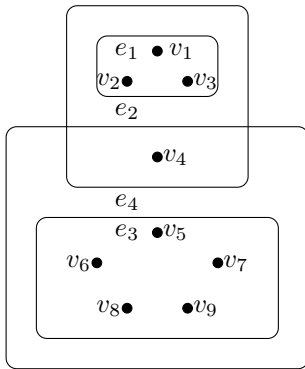


FIGURE 5. Chemical hypergraph.

Example 5.4. This example, which is taken from [23, page-15, figure-13], represents an allylic complex and cyclopropenyl complex. The vertices of the hypergraph are allylic ligands, cyclopropenyl ligands, and metals. Here the hyperedges are the polycentric bonds among the allylic ligands, cyclopropenyl ligands and metals (For detail description of the vertices and hyperedges see [23, Page-14, 15]). The hypergraph contains 9 vertices and 4 hyperedges. This hypergraph is connected because $e_4 \cup e_2$ contains all the vertices and $e_4 \cap e_2$ is non-empty (see Figure 5). Cardinality of $e_1, e_2, e_3,$ and e_4 are 3, 4, 5, and 6 respectively.

Example 5.5. In a google form, a group of peoples are asked the names of social networking websites or applications among Whatsapp, Facebook, Instagram, and hike, used by them. Eight responses are received. Based on those responses, we construct a hypergraph, whose vertices are the persons and hyper-edges are the social networking websites (or applications). Two vertices (persons) are adjacent if they use the same social network application. The hypergraph is connected because V_8 is adjacent to all the other vertices.

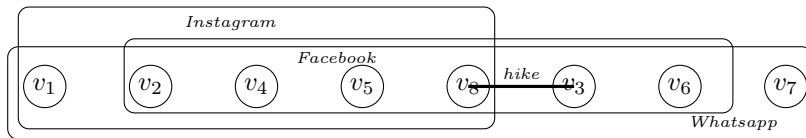


FIGURE 6. hypergraph of social network

Thus, the cardinalities of $e_1, e_2, e_3,$ and e_4 are 8, 6, 5, and 2 respectively.

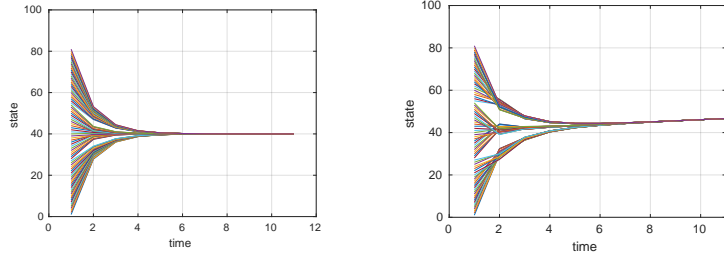
Example 5.6. For this example we consider the set $S = \{2, 3, 4, 5, 6, 8, 9, 10, 12\}$ as the set of vertices of the hypergraph. A hyperedge e_i is the maximal subset of S consists of the elements whose greatest common divisor is $i + 1$, for $i = 1, \dots, 5$. So, two vertices are adjacent in this hypergraph if they have a common divisor (≥ 2). Therefore, the hyperedges are, $e_1 = \{2, 4, 6, 8, 10, 12\}, e_2 = \{3, 6, 9, 12\}, e_3 = \{4, 8, 12\}, e_4 = \{5, 10\}, e_5 = \{6, 12\}$. This hypergraph is connected because e_1, e_2, e_4 cover all the vertices. The incidence matrix of the hypergraph is in the table below.

5.1.2. Simulations on global synchronizability in coupled discrete-time dynamical systems on hypergraphs (un-weighted case).

Example 5.7. In Example 5.1, the hypergraph is a uniform hypergraph. So here $C = B$. The maximum modulus of the eigenvalues of C is $\frac{27}{8}$. Let us choose $\epsilon = 0.5, k = 1, \Gamma = 1$.

With this set up, if we choose $\bar{f}(x) = 20 + \frac{7}{27}x$ and $\bar{g}(x) = 20 + \frac{1}{2}x$, then $[k_g + \epsilon \|C\| k_f \|\Gamma^T\|] < 1$, which is the sufficient condition for synchronization given in Theorem 3.9, Theorem 3.16 and Corollary 3.10 and

Therefore, asymptomatic synchronization of the trajectories of the CDSH is observed (see Figure 7a). If we take $f(x) = g(x) = 1 + 0.99x$ then the maximum modulus of eigenvalues of $(I + \epsilon C) = \|I + \epsilon C\| = 1 < \frac{1}{k_f} = \frac{1}{0.99}$, which is the sufficient condition of synchronization when $f = g$, as given in Theorem 3.9 and Corollary 3.10. Thus, the trajectories synchronize with flow of time (Figure 7b).



(A) Synchronization with $f \neq g$. (B) Synchronization with $f = g$.

FIGURE 7. Sync-trajectories of CDSH with the hypergraph described in Example 5.1 as underlying architecture.

Example 5.8. Consider a CDSH with the underlying hypergraph mentioned in Example 5.5. Here, $\|I + \epsilon C\| = 1.515$, where $\epsilon = 0.5, k = 1$, and $\Gamma = 1$. If we choose $f(x) = g(x) = 2 + \frac{100}{112} \sin x$, then we have $k_f = \frac{100}{112}$ and $\|I + \epsilon C\| k_f > 1$. The sufficient conditions for synchronization given in Theorem 3.9 and Corollary 3.10 are not satisfied and the trajectories remain asynchronous (Figure 8a). When we take $f(x) = g(x) = 2 + \frac{100}{152} x$, then we get $\|I + \epsilon C\| k_f < 1$, and thus, the sufficient conditions for synchronization given in Theorem 3.9 and Corollary 3.10 are satisfied and the trajectories synchronizes asymptotically (Figure 8b).



(A) Behavior of trajectories when $\|I + \epsilon C\| k_f > 1$. (B) Behavior of trajectories when $\|I + \epsilon C\| k_f < 1$.

FIGURE 8. Demonstration of Theorem 3.9 and Corollary 3.10.

Example 5.9. Consider a CDSH with the underlying hypergraph described in Example 5.4. So here $\|I + \epsilon C\| = 1$, where $\epsilon = 0.5, k = 1$, and $\Gamma = 1$. If we choose $f(x) = g(x) = 1 + \frac{3}{2} \cos x$, then $k_f = 1.5$ and $\|I + \epsilon C\| k_f > 1$, but, still the trajectories of the system synchronize globally as stated in Remark 3.12 (see Figure 9). Thus, it is also evident that the conditions stated in Theorem 3.9 and Corollary 3.10 are sufficient but not necessary.

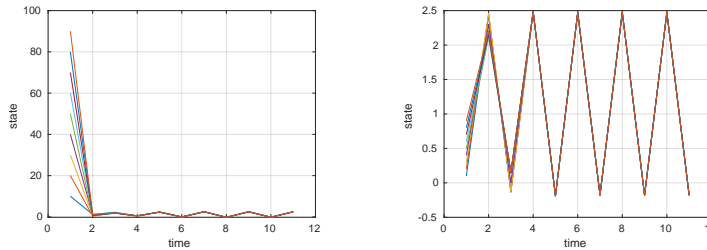
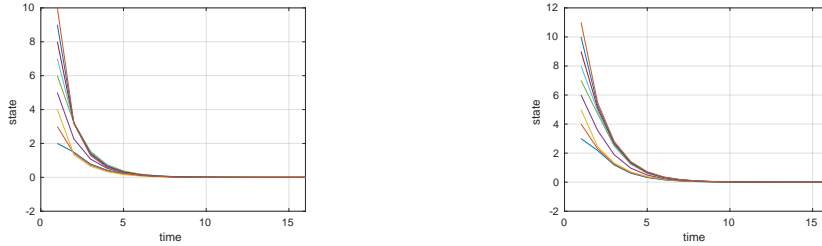


FIGURE 9. Synchronization without satisfying the sufficient conditions.

Example 5.10. Consider a CDSH with $k = 2, \Gamma = \frac{1}{3} I_2, \epsilon = 0.5$, the underlying hypergraph is described in Example 5.4. If we take $\bar{f} : \mathbb{R}^2 \rightarrow \mathbb{R}^2$ is defined by $\begin{pmatrix} x_1 \\ x_2 \end{pmatrix} \mapsto F \begin{pmatrix} x_1 \\ x_2 \end{pmatrix}$, and $\bar{g} : \mathbb{R}^2 \rightarrow \mathbb{R}^2$ is defined as $\begin{pmatrix} x_1 \\ x_2 \end{pmatrix} \mapsto G \begin{pmatrix} x_1 \\ x_2 \end{pmatrix}$, where $F = a \begin{pmatrix} 0 & 1 \\ 1 & 0 \end{pmatrix}$ and $G = b \begin{pmatrix} 3 & 2 \\ 1 & 4 \end{pmatrix}$. Recall Theorem 3.9. So, $k_f = a, k_g = 5b, \|C\| = 2.8333$, and $(k_g + \epsilon \|C\| k_f \|\Gamma^T\|) = (5b + 0.5 \times 2.8333 \times a \times \frac{1}{3})$.

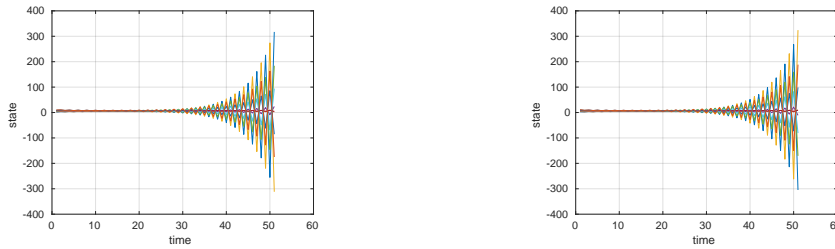
Now if we consider $a = 1$, and $b = \frac{1}{10}$ then $\|C\| = 2.8333$, and $(k_g + \epsilon\|C\|k_f\|\Gamma^T\|) \approx 0.9722 < 1$. Therefore, the sufficient condition, is satisfied and the trajectories synchronize (Figure 10). Here Figure 10a, and Figure 10b show the evolution of the first and second components, respectively, of the dynamics in all the vertices.



(A) The dynamics of the first components of states in all the vertices. (B) The dynamics of the second components of states in all the vertices.

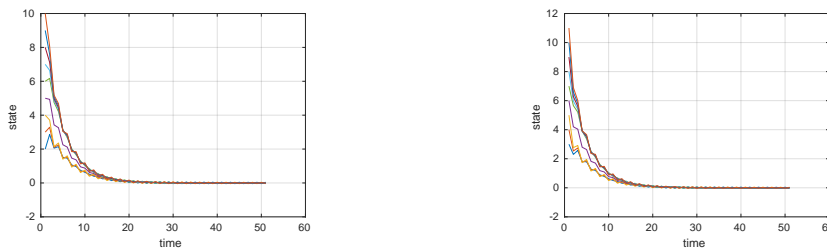
FIGURE 10. Synchronization with $[k_g + \epsilon\|C\|k_f\|\Gamma^T\|] \approx 0.9722 < 1$.

Now if we interchange the functions \bar{f}, \bar{g} and take the other values same, that is, if $\bar{f} : \mathbb{R}^2 \rightarrow \mathbb{R}^2$ is defined by $\begin{pmatrix} x_1 \\ x_2 \end{pmatrix} \mapsto G \begin{pmatrix} x_1 \\ x_2 \end{pmatrix}$, and $\bar{g} : \mathbb{R}^2 \rightarrow \mathbb{R}^2$ is defined by $\begin{pmatrix} x_1 \\ x_2 \end{pmatrix} \mapsto F \begin{pmatrix} x_1 \\ x_2 \end{pmatrix}$ then we get a new CDSH, where $k_g = a$, $k_f = 5b$, and $(k_g + \epsilon\|C\|k_f\|\Gamma^T\|) = (a + 0.5 \times 2.8333 \times 5b \times \frac{1}{3})$. If $a = 1$, and $b = \frac{1}{10}$ then $(k_g + \epsilon\|C\|k_f\|\Gamma^T\|) \approx 1.2 > 1$ and Therefore, the condition of Theorem 3.9 is not satisfied. So synchronization does not happen (see Figure 11). If we take $a = 0.77$, $b = \frac{1}{10}$ then $(k_g + \epsilon\|C\|k_f\|\Gamma^T\|) \approx 1.006 > 1$. Although, here, the condition of Theorem 3.9 is also not satisfied, but, synchronization is achieved (see Figure 12). Thus, the condition provided by Theorem 3.9 is sufficient but not necessary.



(A) The dynamics of the first components of states in all the vertices. (B) The dynamics of the second components of states in all the vertices.

FIGURE 11. Asynchronous trajectories with $[k_g + \epsilon\|C\|k_f\|\Gamma^T\|] \approx 1.2 > 1$.



(A) The dynamics of the first components of states in all the vertices. (B) The dynamics of the second components of states in all the vertices.

FIGURE 12. Synchronization with $[k_g + \epsilon\|C\|k_f\|\Gamma^T\|] \approx 1.006 > 1$.

5.1.3. Simulations for local stability analysis and local synchronizability (with unweighted hypergraph topology).

Example 5.11. Consider a CDSH with $k = 1$, the underlying hypergraph is taken from Example 5.1. If we choose $s_1 = 2$ (defined in Equation (3.22)), and $\bar{f}(x) = \sin x$ then by Equation (3.41), $J_f(n) = \cos(s_{n-1})$, and therefore, $\sigma \approx -0.0053$.

Now if we consider $c = 1$, and $\epsilon = 0.6$ in the condition given in Theorem 3.27, then $[\frac{1-e^{-\sigma}}{c\epsilon}, \frac{1+e^{-\sigma}}{c\epsilon}] = [-0.0088, 3.3422]$. As the underlying hypergraph is taken from Example 5.1, then minimum of absolute values of the nonzero eigenvalue of C is 1.1250 and the maximum of that is 3.3750. As the conditions given in

Corollary 3.31 are satisfied and the required interval is large enough to contain all the absolute values of non zero eigenvalues of C , there is synchronization (Figure 13a) if the initial perturbation is small enough but there may not (Figure 13b) be synchronization if the initial perturbation is not sufficiently small.

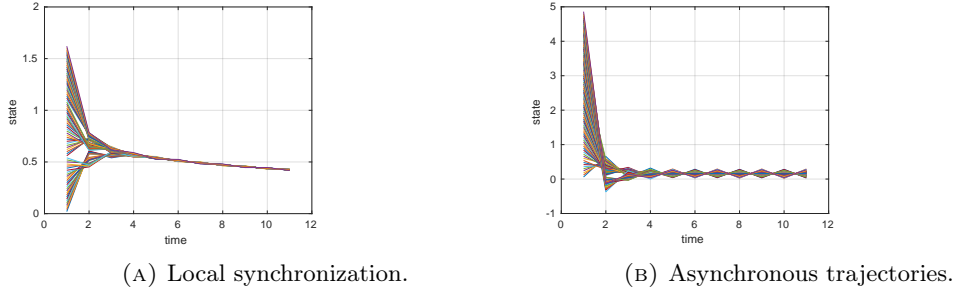


FIGURE 13. Local stability analysis.

Example 5.12. We consider the CDSH with $k = 1$, $s_1 = 2$, and $\bar{f}(x) = \frac{36}{25}x + 5$. Then by Equation (3.41) we have $J_f(n) = \frac{36}{25}$ and therefore, $\sigma \approx 0.3646$. Now if we take $c = 1$ and $\epsilon = 1$ in the conditions of Theorem 3.27, then $[\frac{1-e^{-\sigma}}{c\epsilon}, \frac{1+e^{-\sigma}}{c\epsilon}] = [0.3056, 1.6944]$. If the underlying hypergraph is taken from Example 5.1, then minimum absolute values of the nonzero eigenvalues of C is 1.1250 and the maximum of the same is 3.3750. Thus, the conditions described in Lemma 3.26, Theorem 3.27, and Corollary 3.32 are not satisfied and the trajectories remain asynchronous (Figure 14a).

If we consider $\epsilon = 0.5$, then $[\frac{1-e^{-\sigma}}{c\epsilon}, \frac{1+e^{-\sigma}}{c\epsilon}] = [0.6111, 3.3889]$, and the absolute values of all the nonzero eigenvalues of C contained in this interval and therefore, the trajectories synchronize (Figure 14b).

Now if we take the coupling strength $\epsilon = 0.15$ in the conditions of Theorem 3.27, then $[\frac{1-e^{-\sigma}}{c\epsilon}, \frac{1+e^{-\sigma}}{c\epsilon}] = [2.0370, 11.2963]$. This interval becomes larger but not large enough to contain the absolute values of all the nonzero eigenvalues of C and the trajectories remain asynchronous (Figure 14c).

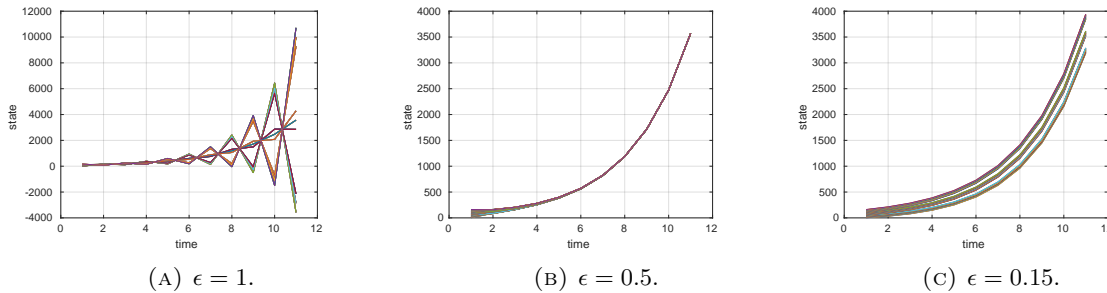


FIGURE 14. Change in local synchronizability with different coupling strengths.

5.1.4. *Examples of coupled dynamical systems on weighted hypergraphs.* In this section we discuss some examples related to weighted systems on hypergraphs and some matrices associated with those systems on hypergraphs.

Example 5.13. Now we construct a weighted systems on hypergraphs where we consider the function of coupling strength $\epsilon : V \rightarrow \mathbb{R}^+$ and the weight function $w : V \rightarrow \mathbb{R}^+$ for edges are the same. The coupling strength of all the edges are $\epsilon_{e_1} = w_{e_1} = \frac{1}{2}$, $\epsilon_{e_2} = w_{e_2} = \frac{3}{5}$, $\epsilon_{e_3} = w_{e_3} = \frac{3}{5}$, $\epsilon_{e_4} = w_{e_4} = \frac{3}{5}$, $\epsilon_{e_5} = w_{e_5} = \frac{1}{2}$, $\epsilon_{e_6} = w_{e_6} = \frac{3}{5}$. The underlying hypergraph taken from Example 5.2.

Example 5.14. Let us consider the hypergraph given in Example 5.3.

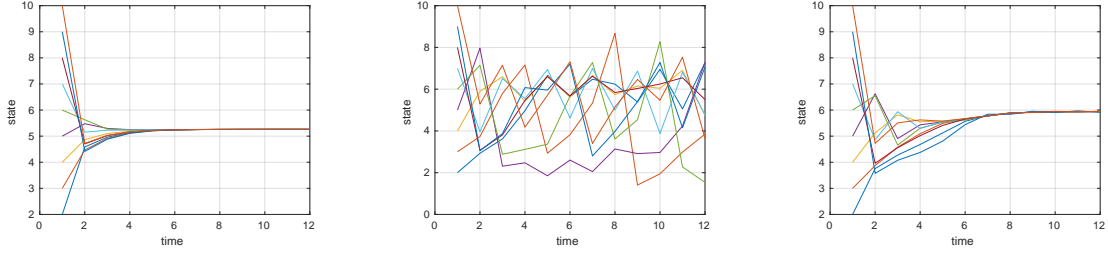
We take the function of coupling strength $\epsilon : V \rightarrow \mathbb{R}^+$ is equal to the weight function $w : V \rightarrow \mathbb{R}^+$ for edges are the same. The coupling strength of all the edges are $\epsilon_{e_1} = w_{e_1} = \frac{3}{10}$, $\epsilon_{e_2} = w_{e_2} = \frac{1}{2}$, $\epsilon_{e_3} = w_{e_3} = \frac{3}{10}$, $\epsilon_{e_4} = w_{e_4} = \frac{1}{2}$, $\epsilon_{e_5} = w_{e_5} = \frac{4}{5}$, $\epsilon_{e_6} = w_{e_6} = \frac{1}{2}$, $\epsilon_{e_7} = w_{e_7} = \frac{3}{10}$, $\epsilon_{e_8} = w_{e_8} = \frac{1}{2}$, and $\epsilon_{e_9} = w_{e_9} = \frac{3}{10}$.

Example 5.15. If we consider the hypergraph from Example 5.5,

We fix $\epsilon_{e_1} = w_{e_1} = 0.3$, $\epsilon_{e_2} = w_{e_2} = 0.5$, $\epsilon_{e_3} = w_{e_3} = 0.3$, and $\epsilon_{e_4} = w_{e_4} = 0.5$.

5.1.5. *Simulations of global synchronization in coupled discrete dynamical systems on hypergraphs.*

Example 5.16. If we consider a weighted discrete CDSH whose underlying hypergraph is the weighted hypergraph considered in Example 5.14. We take $k = 1$, $\Gamma = 1$, $\bar{f}(x) = 5 + \frac{1}{8} \sin x$, and $\bar{g}(x) = 5 + \frac{1}{2} \cos x$. Thus, $\|L_w\| = \mu_{\max} \approx 3.74$ and $(k_g + \|L_w\|k_f\|\Gamma^T\|) = (k_g + \mu_{\max}k_f\|\Gamma^T\|) \approx 0.97 < 1$. Thus, as stated in Theorem 3.41, the trajectories synchronize (Figure 15a).



(A) Synchronization with $(k_g + \|L_w\|k_f\|\Gamma^T\|) < 1$. (B) Asynchronous trajectories with $(k_g + \|L_w\|k_f\|\Gamma^T\|) > 1$. (C) Synchronization with $(k_g + \|L_w\|k_f\|\Gamma^T\|) > 1$.

FIGURE 15. Simulations of effects due the conditions stated in Theorem 3.41 and Corollary 3.42, on synchronization.



(A) Synchronization with $\|I_N + L_w\| \leq \frac{1}{k_f}$. (B) Asynchronous trajectories with $\|I_N + L_w\| \geq \frac{1}{k_f}$.

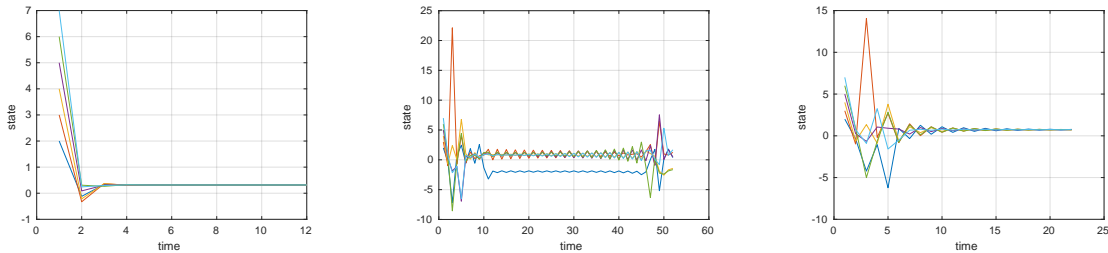
FIGURE 16. Simulation of effects due the conditions given in Theorem 3.41 and Corollary 3.42, for $f = g$.

If we take $\bar{f}(x) = 5 + \sin x$ and $\bar{g}(x) = 5 + \cos x$, then $(k_g + \|L_w\|k_f\|\Gamma^T\|) \approx 4.74 > 1$ and the trajectories remain asynchronous (see Figure 15b).

The conditions given in Theorem 3.41 and Corollary 3.42 are sufficient conditions of synchronization, but not necessary. Therefore, synchronization may happen without complying with those conditions. As an example, take $\bar{f}(x) = \frac{1}{2} \sin x$ and $\bar{g}(x) = \cos x$ in the above example (Figure 15c).

With the above set up, we consider $f = g$ and $\bar{f}(x) = \bar{g}(x) = a \sin x$. Thus, we have $\|I_N + L_w\| = \omega \approx 2.74$ and $k_f = a$. Now if we consider $a = \frac{1}{3}$, which shows $\|I_N + L_w\| = \omega \approx 2.74 < 3 = \frac{1}{k_f}$, then the sufficient condition of Theorem 3.41 and Corollary 3.42 is satisfied and synchronization is observed (see Figure 16a). If we take $a = \frac{1}{2}$, which implies $\|I_N + L_w\| = \omega \approx 2.74 > 2 = \frac{1}{k_f}$, i.e., there is no synchronization (see Figure 16b).

Example 5.17. If we consider the CDSH, with the underlying weighted hypergraph is chosen from Example 5.13. Take $k = 1, \Gamma = 1, \bar{f}(x) = a \frac{x}{1+x}, \bar{g}(x) = b \cos x$, which implies $\|L_w\| \approx 2.93 \implies (\|sup\bar{g}'\| + \|\Gamma^T\| \|L_w\| \|sup\bar{f}'\|) \approx (b + 2.93a)$. Now if we consider $a = \frac{1}{5}$ and $b = \frac{1}{3}$, then we get $(\|sup\bar{g}'\| + \|\Gamma^T\| \|L_w\| \|sup\bar{f}'\|) \approx 0.92 < 1$, complying with the sufficient condition of Theorem 3.45 and Therefore, the trajectories synchronize (Figure 17a). If we take $a = \frac{3}{2}, b = 1$, then $(\|sup\bar{g}'\| + \|\Gamma^T\| \|L_w\| \|sup\bar{f}'\|) \approx 5.40 > 1$, is not complying with the sufficient condition and the trajectories remain asynchronous (Figure 17b). If $a = \frac{1}{2}$ and $b = 1$, then $(\|sup\bar{g}'\| + \|\Gamma^T\| \|L_w\| \|sup\bar{f}'\|) \approx 2.46 > 1$. Although, here, it is not complying with the condition, but trajectories synchronize (see Figure 17c). Thus, it indicates that the condition is sufficient but not necessary.



(A) Synchronization with $(\|sup\bar{g}'\| + \|\Gamma^T\| \|L_w\| \|sup\bar{f}'\|) < 1$. (B) Asynchronous trajectories with $(\|sup\bar{g}'\| + \|\Gamma^T\| \|L_w\| \|sup\bar{f}'\|) > 1$. (C) Synchronization with $(\|sup\bar{g}'\| + \|\Gamma^T\| \|L_w\| \|sup\bar{f}'\|) > 1$.

FIGURE 17. Simulations of effects of the conditions given in Theorem 3.41 and Corollary 3.42, on synchronization.

Example 5.18. If we consider an weighted discrete CDSH whose underlying weighted hypergraph is taken from Example 5.14. Choose $k = 1$, $\Gamma = 1$, $\bar{g}(x) = \bar{f}(x) = px + q \sin x$, then we have $\|[I_N + L_w]\| \approx 2.74$ and $\frac{1}{\|\sup \bar{f}'\|} = \frac{1}{p+q}$. This shows that the condition given in Corollary 3.46 is satisfied when $2.74 < \frac{1}{p+q}$. Now if we take $p = \frac{5}{27}, q = \frac{4}{27}$, then $\|[I_N + L_w]\| \|\sup \bar{f}'\| \approx 2.74 \times \frac{9}{27} = 0.91 < 1$, complying with the sufficient condition of Corollary 3.46, Therefore, the trajectories synchronize (Figure 18a). If we choose $p = \frac{5}{27}, q = \frac{6}{27}$, then $\|[I_N + L_w]\| \|\sup \bar{f}'\| \approx 2.74 \times \frac{11}{27} \approx 1.11 > 1$, which does not satisfy the sufficient condition of Corollary 3.46, and thus, the trajectories remain asynchronous (Figure 18b).

If we consider $p = \frac{5}{27}$, and $q = \frac{5}{27}$, which implies $\|[I_N + L_w]\| \|\sup \bar{f}'\| \approx 2.74 \times \frac{10}{27} \approx 1.0155 > 1$. Although, it does not comply with the sufficient condition of Corollary 3.46, the trajectories synchronize (Figure 18c), and which shows that the condition is sufficient, but not necessary.

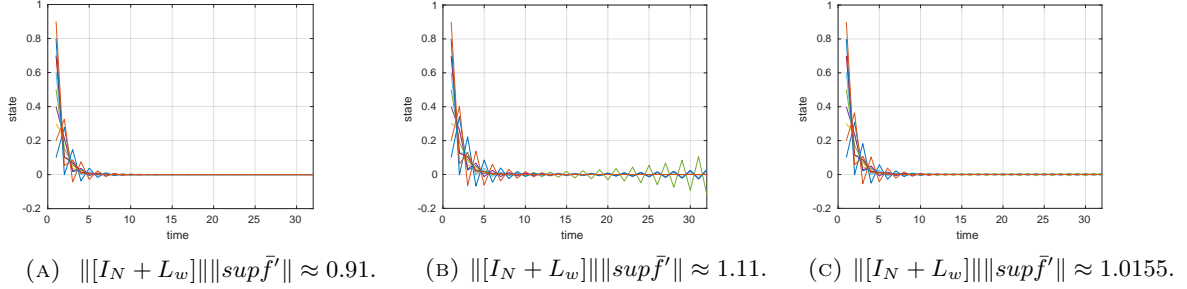


FIGURE 18. Simulations of effects of the conditions given in Theorem 3.41 and Corollary 3.42, on synchronization.

5.1.6. Simulations of the results on local synchronization of coupled discrete dynamical systems on weighted hypergraphs.

Example 5.19. If we consider the CDSH, where the underlying weighted hypergraph is taken from Example 5.15. Choose $k = 1$, $\Gamma = 1$, and $\bar{g}(x) = \bar{f}(x) = e^{p \sin \frac{x}{q}}$. Then for $p = 1, q = 1$ we have $\sigma \approx -1.0578$ and $[(1 - e^{-\sigma}), (1 + e^{-\sigma})] \approx [-1.88, 3.88]$, and thus, the maximum and minimum of the absolute values of the eigenvalues of L_w are 2.1268 and 0, respectively. So the condition given in Corollary 3.50 is satisfied and the trajectories synchronize (Figure 19a) if the perturbation is sufficiently small.

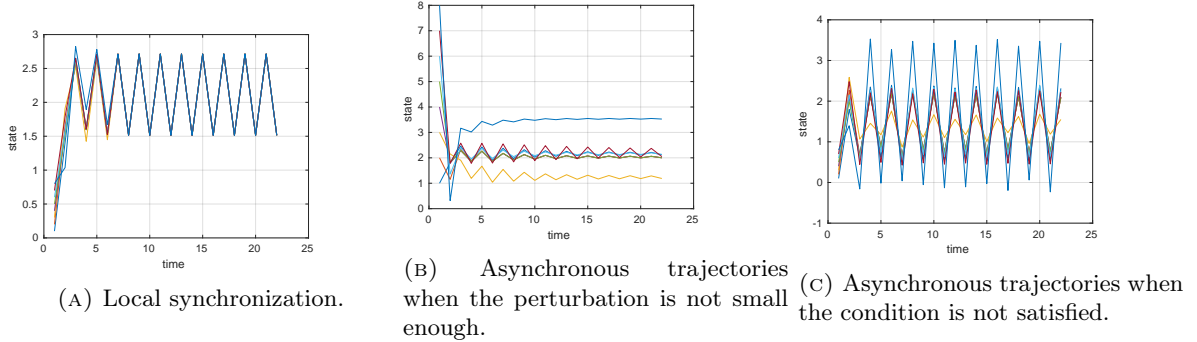


FIGURE 19. Simulations of Corollary 3.50 on local synchronization.

Note that Corollary 3.50 is a result on local synchronization. Thus, if the perturbation is not small enough there may not be synchronization (Figure 19b) in spite of complying with the condition given in Corollary 3.50. In the above example, if we keep all the conditions same, but set the initial condition little far from the synchronization manifold then the trajectories remain asynchronous (Figure 19c). If we take $p = 1, q = \frac{1}{2}$, then we have $[(1 - e^{-\sigma}), (1 + e^{-\sigma})] \approx [-0.0547, 2.0547]$, which does not comply with the condition, and thus, in spite of very small perturbation the trajectories remain asynchronous.

5.1.7. Simulations of coupled continuous-time dynamical systems on hypergraphs model.

Example 5.20. Take the hypergraph given in Example 5.15 as the underlying hypergraph. Choose $k = 1$, $\Gamma = 1$, and $\bar{f} = -ax + b, \bar{g} = cx + d$. Thus, $\frac{d\bar{f}(s_t)}{dt} = -a$ and $\frac{d\bar{g}(s_t)}{dt} = b$. Now if we take $b = a > 0$ and $c > 0$ then $(\frac{d\bar{f}(s_t)}{dt} + \mu_i \frac{d\bar{g}(s_t)}{dt} + b) \leq 0$ for all t, i and Therefore, the trajectories synchronize. For example if we choose $a = 0.2, c = 0.1$ then the condition given in Corollary 3.62 is satisfied and the trajectories synchronize (Figure 20a). For $a = -0.2, c = 0.1$ the condition of Corollary 3.62 is not satisfied and the trajectories

remain asynchronous (Figure 20b). When $a = -0.2, c = 3$, despite not satisfying the condition, the trajectories synchronize (Figure 20c), and which shows that the condition is sufficient but not necessary.

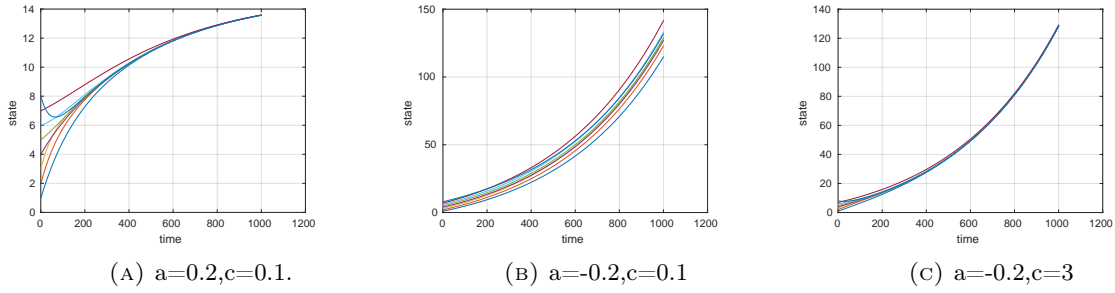


FIGURE 20. Simulation of Corollary 3.62 on local synchronization.

5.2. Chemical-gene interaction (biogrid) and protein complex hypergraphs. Now we extend our study on two hypergraphs, (i) biogrid hypergraph and (ii) protein-complex hypergraph, which are created from real data. Biogrid hypergraph is constructed from human chemical-gene(target) interactions which are useful for studying drug-gene(target) interactions (The data is downloaded on 18/02/2019 from the repository, BioGRID [12]). Here the genes are considered as vertices, and chemicals are as hyperedges. A hyperedge corresponding to a chemical is constituted by a group of genes that are targeted by that chemical. Protein complex hypergraph is created from the database, CORUM [20], a resource of mammalian protein complexes (the data is also downloaded on 18/02/2019) and which is also useful for predicting unknown interactions between proteins. Here protein complexes are considered as vertices and subunits are as hyperedges. A hyperedge(subunit) is constructed with the protein complex associated with the corresponding subunit. Initially, the biogrid hypergraph contained 2138 vertices and 4455 hyperedges, whereas the protein complex hypergraph was made of 3638 vertices and 2848 hyperedges. After removing all the hyperedges containing only one vertex, we find 1501 hyperedges in our biogrid hypergraph. Since our theoretical results are on connected hypergraph, we use the largest connected component as the underlying topology of dynamical networks in our study. The largest connected component of the biogrid hypergraph consists of 1808 vertices and 1431 hyperedges. The same of the protein complex hypergraph contains 2770 vertices and 2383 hyperedges.

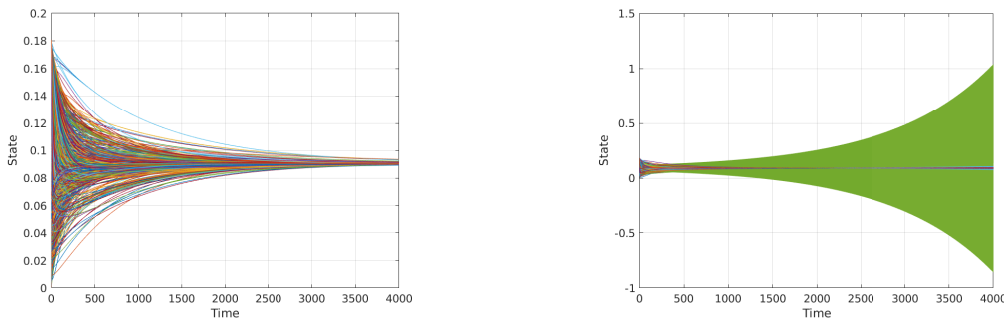
5.2.1. *Comparison with the hypergraph and its underlying graph.* Now we consider the diffusion equations,

$$x(n+1) = x(n) + \frac{1}{110}C(x(n)) \quad (5.1)$$

involving the diffusion operator C , and

$$x(n+1) = x(n) + \frac{1}{110}L(x(n)) \quad (5.2)$$

containing the negative Laplacian of the underlying graph of the biogrid hypergraph.



(A) Trajectories of the dynamical system given by Equation (5.1). (B) Trajectories of the dynamical system given by Equation (5.2).

FIGURE 21. Comparison with the hypergraph and its underlying graph in Chemical-gene interaction (biogrid) hypergraph.

The converging evolution of the trajectories (fig. 21a) given by Equation (5.1) demonstrates the presence of a diffusion process in the dynamical system. In contrast, the evolution of the trajectories given by Equation (5.2) is divergence in nature (fig. 21b). Therefore, for biogrid hypergraph, C is a better diffusion operator than L . To have another instance where C is proved to be a better diffusion operator than the negative laplacian L of

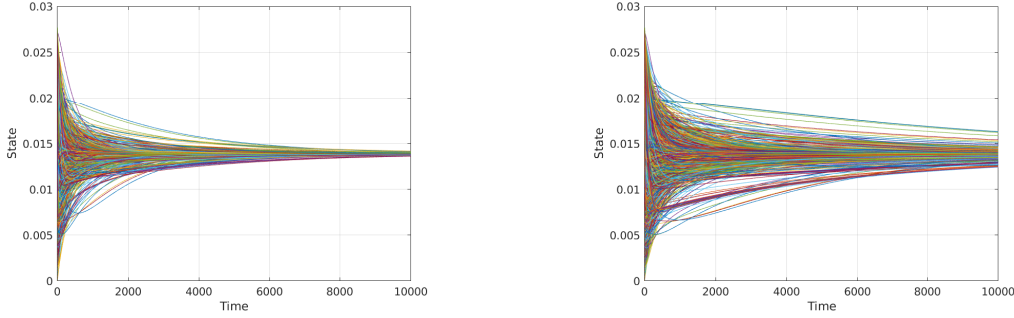
the underlying graph of the same hypergraph, we present one more comparison. Consider the following discrete diffusion equations

$$x(n+1) = x(n) + \frac{1}{200}C(x(n)) \quad (5.3)$$

involving the diffusion operator C of the protein complex hypergraph and

$$x(n+1) = x(n) + \frac{1}{200}L(x(n)) \quad (5.4)$$

involving the negative Laplacian of the underlying graph of the protein complex hypergraph. Considering the 10000 iterations in the trajectories of the dynamical system given by Equation (5.3) (Figure 22a) and Equation (5.4) (Figure 22b), it is clear that the trajectories of system given by Equation (5.3) converging faster than that of the system given by Equation (5.4).

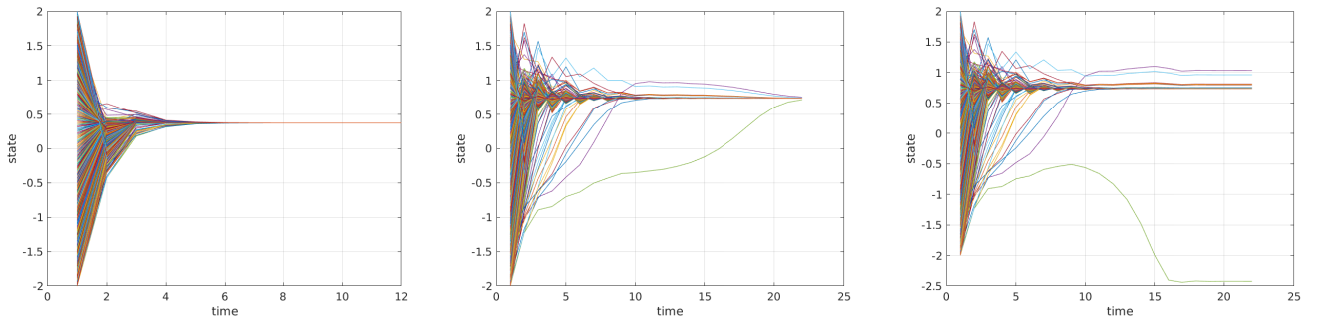


(A) Trajectories of the dynamical system given by Equation (5.3) (B) Trajectories of the dynamical system given by Equation (5.4).

FIGURE 22. Comparison with the hypergraph and its underlying graph in protein complex hypergraph.

5.2.2. *Global analysis of synchronization in dynamical networks with biogrid hypergraph topology.* In this section we will verify our theoretical results on global synchronization with some dynamical networks with the biogrid hypergraph as its underlying architecture.

Example 5.21. *In this example we consider the dynamical network given by Equation (3.16) with the biogrid hypergraph as its underlying topology. We set $k = 1, \Gamma = 1$. If we define $f : \mathbb{R} \rightarrow \mathbb{R}$ as $x \mapsto q \sin(-x)$ and $\bar{g} : \mathbb{R} \rightarrow \mathbb{R}$ as $x \mapsto p \cos(-x)$ then the lipschitz constants $k_g = p, k_f = q$. If we choose $\epsilon = \frac{1}{88}$ and $p = 0.4, q = 0.5$ then $[k_g + \epsilon \|C\| \|k_f\| \|\Gamma^T\|] = (p + \frac{1}{88}(87.6182)q) < 1$, which is the condition given in Theorem 3.9, Theorem 3.16. Thus, the trajectories of the dynamical network synchronizes (Figure 23a). If we choose $p = 1, q = 1.53$, then the condition given in Theorem 3.9, Theorem 3.16 does not satisfied and the trajectories remain asynchronous (Figure 23c). If $p = 1, q = 1.52$ then $[k_g + \epsilon \|C\| \|k_f\| \|\Gamma^T\|] > 1$ that is the conditions of Theorem 3.9, Theorem 3.16 are not satisfied. In spite of that the trajectories synchronizes (Figure 23b). This shows that the condition is sufficient but not necessary.*



(A) Synchronization with $[k_g + \epsilon \|C\| \|k_f\| \|\Gamma^T\|] < 1$. (B) Synchronization with $[k_g + \epsilon \|C\| \|k_f\| \|\Gamma^T\|] > 1$. (C) Asynchronous trajectories with $[k_g + \epsilon \|C\| \|k_f\| \|\Gamma^T\|] > 1$.

FIGURE 23. Simulation of Theorem 3.9, Theorem 3.16.

Example 5.22. *In this example we consider the dynamical network given by Equation (3.16) with the biogrid hypergraph as its underlying topology. If the coupling strength $\epsilon = \frac{1}{45}$, $k = 1, \Gamma = 1$ then $\|[I_N + \epsilon C]\| = 1$. Now*

if we define $\bar{f} = \bar{g} : \mathbb{R} \rightarrow \mathbb{R}$ as $x \mapsto qe^{\sin x}$, then $k_f = k_g = \sup \left\| \frac{d}{dx}(\bar{f}(x)) \right\| = \sup \|(q \cos(x)e^{\sin(x)})\| \leq qe$. Therefore, if we choose $q = \frac{1}{2.8} < \frac{1}{e}$ then $\|I + \epsilon C\| < \frac{1}{k_f}$ and $\|I_N + \epsilon C\| < \frac{1}{\|\sup \bar{f}'\|}$ which are the condition given in Theorem 3.9, Corollary 3.17. Therefore, the trajectories synchronize (Figure 24a). Calculating in Matlab we get $k_f = k_g = \sup \left\| \frac{d}{dx}(\bar{f}(x)) \right\| = \sup \|(q \cos(x)e^{\sin(x)})\| \approx q \times 1.46$. Thus, if we choose $q = \frac{1}{1.47}$, it agrees with the condition given in given in Theorem 3.9, Corollary 3.17. Therefore, the trajectories synchronize (Figure 24b). When $q = \frac{1}{1.15}$, the condition given in Theorem 3.9, Corollary 3.17 is not satisfied and the trajectories remain asynchronous (Figure 24c). However, if $q = \frac{1}{1.15}$ then also the condition is not satisfied but synchronization is observed in this case (Figure 24d). This is because the condition is sufficient but not necessary.

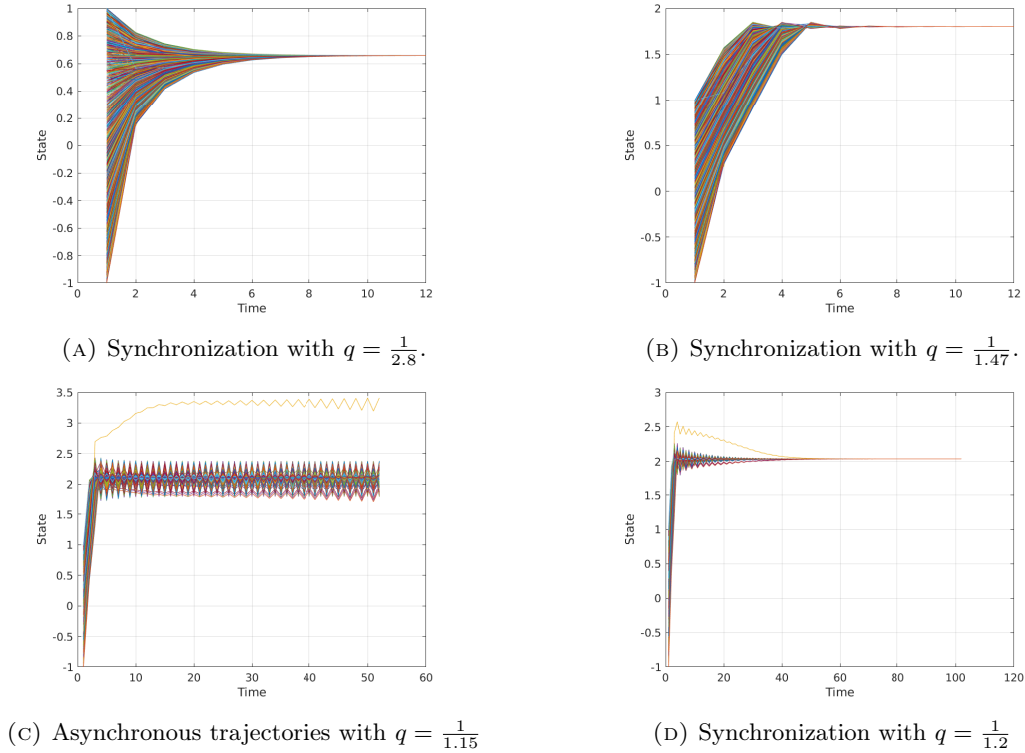
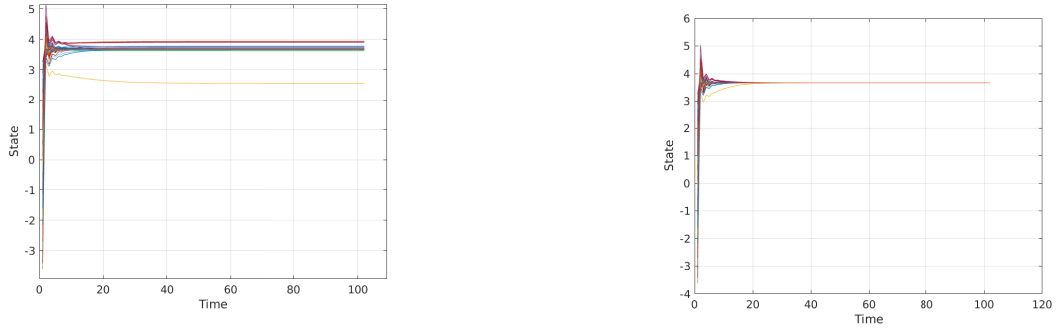


FIGURE 24. Simulation of Theorem 3.9, Corollary 3.17.

5.2.3. Local stability analysis of synchronization in discrete time CDSH with the real hypargraphs.

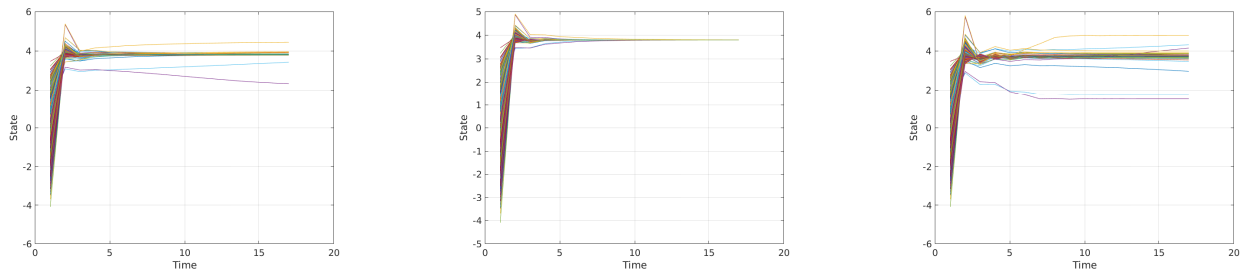
Example 5.23. In this example we consider the dynamical network given by Equation (3.16) with the biogrid hypergraph as its underlying topology. We also choose $k = 1, \Gamma = 1$ and $\bar{f} = \bar{g} : \mathbb{R} \rightarrow \mathbb{R}$ defined as $x \mapsto q \sin x$. Now if we choose $\epsilon = \frac{1}{33}$, then $[\frac{1-e^{-\sigma}}{\epsilon}, \frac{1+e^{-\sigma}}{\epsilon}] = [-16.5, 82.5]$, which is not large enough to contains the absolute values of all the non zero eigenvalues of C . Therefore, the synchronized state is not reached (Figure 25a). However, if we choose $\epsilon = \frac{1}{36}$, then $[\frac{1-e^{-\sigma}}{\epsilon}, \frac{1+e^{-\sigma}}{\epsilon}] = [-18, 90]$, which contains the absolute values of all the eigenvalues of C . Thus, synchronized state is reached (Figure 25b).

Example 5.24. In this example we consider the dynamical network given by Equation (3.16) with the protein complex hypergraph as its underlying topology. We also choose $k = 1, \Gamma = 1$ and $\bar{f} = \bar{g} : \mathbb{R} \rightarrow \mathbb{R}$ defined as $x \mapsto q \sin x$. Now if we choose $q = \frac{1}{3}$, then $[\frac{1-e^{-\sigma}}{\lambda_{\min}}, \frac{1+e^{-\sigma}}{\lambda_{\max}}] \approx [-151.52, 0.0526]$. Therefore, if we choose $\epsilon = 0.07$ the synchronized state is not reached (Figure 26a). However, if we choose $\epsilon = 0.05$, then synchronized state is reached (Figure 26b). However, when $q = \frac{1}{1.5}$ and $\epsilon = 0.05$ the trajectories remain asynchronous because $\epsilon = 0.05 \notin [\frac{1-e^{-\sigma}}{\lambda_{\min}}, \frac{1+e^{-\sigma}}{\lambda_{\max}}] \approx [-37.8788, 0.0329]$ (Figure 26c).



(A) Asynchronous trajectories with $[\frac{1-e^{-\sigma}}{\epsilon}, \frac{1+e^{-\sigma}}{\epsilon}] = [-16.5, 82.5]$. (B) Synchronization with $[\frac{1-e^{-\sigma}}{\epsilon}, \frac{1+e^{-\sigma}}{\epsilon}] = [-18, 90]$.

FIGURE 25. Local stability analysis of synchronization in discrete time CDSH with biogrid hypergraph.



(A) Asynchronous trajectories with $[\frac{1-e^{-\sigma}}{\lambda_{\min}}, \frac{1+e^{-\sigma}}{\lambda_{\max}}] \approx [-151.52, 0.0526]$, $q = \frac{1}{3}$, $\epsilon = 0.07$. (B) Synchronization with $[\frac{1-e^{-\sigma}}{\lambda_{\min}}, \frac{1+e^{-\sigma}}{\lambda_{\max}}] \approx [-151.52, 0.0526]$, $q = \frac{1}{3}$, $\epsilon = 0.05$. (C) Asynchronous trajectories with $[\frac{1-e^{-\sigma}}{\lambda_{\min}}, \frac{1+e^{-\sigma}}{\lambda_{\max}}] \approx [-37.88, 0.033]$, $q = \frac{2}{3}$, $\epsilon = 0.05$.

FIGURE 26. Local stability analysis of synchronization in discrete time CDSH with the protein complex hypergraph.

6. CONCLUSION

We have introduced a new class of dynamical networks capable of throwing light on multi-body interactions among a group of arbitrary sizes. Naturally, some traditional dynamical network with its binary interaction becomes a subclass of our models. We have presented analytic perspectives of synchronization in a dynamical network with multi-body interactions. We have also proved that some old results on the synchronization in dynamical networks with pairwise interactions are also valid for the same in the multi-body interaction framework. Besides that, some new results on synchronization are also provided. Moreover, our study has found some operators which can incorporate diffusive interactions among arbitrarily large groups of agents. The huge volume of literature involving complex systems and dynamical networks with traditional graph architecture shows that our proposed multi-nary framework has a large scope of applications and further developments. Our study indicates that many well-studied facts of binary interaction framework also hold for the proposed multi-nary framework.

In Section 3.3, we have observed that the lower bounds and upper bounds of the absolute values of the eigenvalues of the diffusion operators associated with the underlying hypergraph yield sufficient conditions for local synchronization. Thus, finding better bounds of the same will lead us to better sufficient conditions for local synchronization. In this study, we have always considered that the underlying hypergraph is undirected and thus, the diffusion matrices are symmetric and which makes our study simple. The diffusion matrices related to a directed dynamical network may not be symmetric. So the study of synchronization in directed systems on hypergraphs will be interesting.

ACKNOWLEDGEMENTS

The authors would like to show their gratitude to Shirshendu Chowdhury for his constant valuable advice and guidance for studying dynamical systems throughout this work. His constructive comments have enriched this study enormously. The authors are also grateful to Timoteo Carletti for helpful discussions on the terminologies, hyper-networks, and hypergraphs.

The authors are sincerely thankful to Meghna, Chiranjee Ghosh, Sourav Makhil, Saikat Mondal, Buddhadev Chatterjee, Kausik Das, Arun Sardar for their precious responses in a google form, that help us to construct the hypergraph of Example 5.5. The authors are also thankful to Mrinmay Biswas, Sugata Ghosh, Gargi Ghosh, Avishek Chatterjee, Shibananda Biswas, and Somnath Basu for fruitful discussions.

The work of second author is supported by University Grants Commission, India (Beneficiary Code/Flag: BININ00965055 A).

REFERENCES

- [1] M. ABUFOUDA AND K. A. ZWEIG, *A theoretical model for understanding the dynamics of online social networks decay*, arXiv preprint arXiv:1610.01538, (2016). 1
- [2] R. ALBERT AND A.-L. BARABÁSI, *Statistical mechanics of complex networks*, Reviews of modern physics, 74 (2002), p. 47. 1
- [3] A. ARENAS, A. DÍAZ-GUILERA, J. KURTHS, Y. MORENO, AND C. ZHOU, *Synchronization in complex networks*, Physics reports, 469 (2008), pp. 93–153. 2
- [4] A. BANERJEE, *On the spectrum of hypergraphs*, Linear Algebra and its Applications, (2020). 3, 18
- [5] A. BANERJEE, A. CHAR, AND B. MONDAL, *Spectra of general hypergraphs*, Linear Algebra and its Applications, 518 (2017), pp. 14–30. 3
- [6] A.-L. BARABASI AND Z. N. OLTVAI, *Network biology: understanding the cell's functional organization*, Nature reviews genetics, 5 (2004), pp. 101–113. 1
- [7] A. R. BENSON, R. ABEBE, M. T. SCHAUB, A. JADBABAIE, AND J. KLEINBERG, *Simplicial closure and higher-order link prediction*, Proceedings of the National Academy of Sciences, 115 (2018), pp. E11221–E11230. 1
- [8] D. BEYSENS AND G. FORGACS, *Dynamical Networks in Physics and Biology: At the Frontier of Physics and Biology Les Houches Workshop, March 17–21, 1997*, vol. 10, Springer Science & Business Media, 2013. 1
- [9] N. BOF, R. CARLI, AND L. SCHENATO, *Lyapunov theory for discrete time systems*, arXiv preprint arXiv:1809.05289, (2018). 14
- [10] S. BOYD, L. EL GHAOU, E. FERON, AND V. BALAKRISHNAN, *Linear matrix inequalities in system and control theory*, vol. 15, Siam, 1994. 14
- [11] K. M. CARLEY, J. PFEFFER, H. LIU, F. MORSTATTER, AND R. GOOLSBY, *Near real time assessment of social media using geo-temporal network analytics*, in Proceedings of the 2013 IEEE/ACM International Conference on Advances in Social Networks Analysis and Mining, 2013, pp. 517–524. 1
- [12] A. CHATR-ARYAMONTRI, R. OUGHTRED, L. BOUCHER, J. RUST, C. CHANG, N. K. KOLAS, L. O'DONNELL, S. OSTER, C. THEESFELD, A. SELAM, ET AL., *The biogrid interaction database: 2017 update*, Nucleic acids research, 45 (2017), pp. D369–D379. 30
- [13] J. CHEN, J.-A. LU, C. ZHAN, AND G. CHEN, *Laplacian spectra and synchronization processes on complex networks*, in Handbook of Optimization in Complex Networks, Springer, 2012, pp. 81–113. 2
- [14] B. L. CLARKE, *Theorems on chemical network stability*, The Journal of Chemical Physics, 62 (1975), pp. 773–775. 1
- [15] K. CZOLCZYNSKI, P. PERLIKOWSKI, A. STEFANSKI, AND T. KAPITANIAK, *Huygens'odd sympathy experiment revisited*, International Journal of Bifurcation and Chaos, 21 (2011), pp. 2047–2056. 1
- [16] M. DE DOMENICO, A. SOLÉ-RIBALTA, E. COZZO, M. KIVELÄ, Y. MORENO, M. A. PORTER, S. GÓMEZ, AND A. ARENAS, *Mathematical formulation of multilayer networks*, Physical Review X, 3 (2013), p. 041022. 2
- [17] P. DELELLIS, M. DI BERNARDO, AND G. RUSSO, *On quad, lipschitz, and contracting vector fields for consensus and synchronization of networks*, IEEE Transactions on Circuits and Systems I: Regular Papers, 58 (2010), pp. 576–583. 20
- [18] S. N. DOROGOVTSSEV AND J. F. MENDES, *Evolution of networks*, Advances in physics, 51 (2002), pp. 1079–1187. 1
- [19] M. FRASCA, L. V. GAMBUZZA, A. BUSCARINO, AND L. FORTUNA, *Synchronization in Networks of Nonlinear Circuits: Essential Topics with MATLAB® Code*, Springer, 2018. 2
- [20] M. GIURGIU, J. REINHARD, B. BRAUNER, I. DUNGER-KALTENBACH, G. FOBO, G. FRISHMAN, C. MONTRONE, AND A. RUEPP, *Corum: the comprehensive resource of mammalian protein complexes—2019*, Nucleic acids research, 47 (2019), pp. D559–D563. 30
- [21] A. N. GORBAN, N. JARMAN, E. STEUR, C. VAN LEEUWEN, AND I. Y. TYUKIN, *Leaders do not look back, or do they?*, Mathematical Modelling of Natural Phenomena, 10 (2015), pp. 212–231. 1
- [22] J. JOST AND M. P. JOY, *Spectral properties and synchronization in coupled map lattices*, Physical Review E, 65 (2001), p. 016201. 4, 5, 14, 15, 22
- [23] E. KONSTANTINOVA, *Chemical hypergraph theory. pohang univ, Sci. Tech, Pohang, (2001)*. 24

- [24] C. LI AND G. CHEN, *Synchronization in general complex dynamical networks with coupling delays*, Physica A: Statistical Mechanics and its Applications, 343 (2004), pp. 263–278. [4](#), [5](#), [14](#), [15](#)
- [25] T. LIU, D. J. HILL, AND J. ZHAO, *Synchronization of dynamical networks by network control*, IEEE Transactions on Automatic Control, 57 (2011), pp. 1574–1580. [2](#), [15](#)
- [26] X. LIU AND K. ZHANG, *Synchronization of linear dynamical networks on time scales: Pinning control via delayed impulses*, Automatica, 72 (2016), pp. 147–152.
- [27] J. LU AND G. CHEN, *A time-varying complex dynamical network model and its controlled synchronization criteria*, IEEE Transactions on Automatic Control, 50 (2005), pp. 841–846. [2](#)
- [28] W. LU, F. M. ATAY, AND J. JOST, *Synchronization of discrete-time dynamical networks with time-varying couplings*, SIAM Journal on Mathematical Analysis, 39 (2008), pp. 1231–1259. [4](#), [5](#), [15](#)
- [29] W. LU AND T. CHEN, *Synchronization analysis of linearly coupled networks of discrete time systems*, Physica D: Nonlinear Phenomena, 198 (2004), pp. 148–168. [14](#)
- [30] ———, *New approach to synchronization analysis of linearly coupled ordinary differential systems*, Physica D: Nonlinear Phenomena, 213 (2006), pp. 214–230. [20](#)
- [31] S. C. MANRUBIA, A. S. MIKHAILOV, ET AL., *Emergence of dynamical order: synchronization phenomena in complex systems*, World Scientific, 2004. [2](#)
- [32] R. MULAS, C. KUEHN, AND J. JOST, *Coupled dynamics on hypergraphs: Master stability of steady states and synchronization*, arXiv preprint arXiv:2003.13775, (2020). [2](#)
- [33] M. E. NEWMAN, *The structure and function of complex networks*, SIAM review, 45 (2003), pp. 167–256. [1](#)
- [34] A. PATANIA, G. PETRI, AND F. VACCARINO, *The shape of collaborations*, EPJ Data Science, 6 (2017). [1](#)
- [35] G. PETRI AND A. BARRAT, *Simplicial activity driven model*, Physical review letters, 121 (2018), p. 228301. [1](#)
- [36] G. PETRI, P. EXPERT, F. TURKHEIMER, R. CARHART-HARRIS, D. NUTT, P. J. HELLYER, AND F. VACCARINO, *Homological scaffolds of brain functional networks*, Journal of The Royal Society Interface, 11 (2014), p. 20140873. [1](#)
- [37] M. PORFIRI AND M. FRASCA, *Robustness of synchronization to additive noise: how vulnerability depends on dynamics*, IEEE Transactions on Control of Network Systems, 6 (2018), pp. 375–387. [2](#), [15](#)
- [38] L. QI AND Z. LUO, *Tensor analysis: spectral theory and special tensors*, SIAM, 2017. [11](#)
- [39] S. RAKSHIT, B. K. BERA, E. M. BOLLT, AND D. GHOSH, *Intralayer synchronization in evolving multiplex hypernetworks: Analytical approach*, SIAM Journal on Applied Dynamical Systems, 19 (2020), pp. 918–963. [2](#)
- [40] G. RANGARAJAN AND M. DING, *Stability of synchronized chaos in coupled dynamical systems*, Physics Letters A, 296 (2002), pp. 204–209. [4](#), [5](#), [15](#)
- [41] A. SARKAR AND A. BANERJEE, *Joins of hypergraphs and their spectra*, Linear Algebra and its Applications, (2020). [14](#), [15](#)
- [42] F. SORRENTINO, *Synchronization of hypernetworks of coupled dynamical systems*, New Journal of Physics, 14 (2012), p. 033035. [2](#)
- [43] S. H. STROGATZ, *Exploring complex networks*, nature, 410 (2001), pp. 268–276. [1](#)
- [44] A. R. WILLMS, P. M. KITANOV, AND W. F. LANGFORD, *Huygens’ clocks revisited*, Royal Society Open Science, 4 (2017), p. 170777. [1](#)
- [45] X. WU, X. ZHAO, J. LÜ, L. TANG, AND J. LU, *Identifying topologies of complex dynamical networks with stochastic perturbations*, IEEE Transactions on Control of Network Systems, 3 (2016), pp. 379–389. [1](#)
- [46] Z. WU, J. DUAN, AND X. FU, *Synchronization of an evolving complex hyper-network*, Applied Mathematical Modelling, 38 (2014), pp. 2961–2968. [2](#)